A Computational Investigation of Solid Electrolyte Materials Using First Principles and Machine Learning Methodologies

Public Talk for PhD Defense

D. Cory Lynch

Wednesday July 29, 2026

ZSR Library Room 404

Acknowledgments

- Dr. Natalie Holzwarth, Wake Forest University – Advisor
- Dr. Fan Yang, Wake Forest University – Committee chair
- Dr. Samuel Cho, Wake Forest University – Committee member
- Dr. Timo Thonhauser, Wake Forest University – Committee member
- Dr. Stephen Winter, Wake Forest University – Committee member
- Dr. Yan Li, National University of Singapore – Coauthor
- Chuin Wei Tan, Harvard University – Coauthor
- Dr. Sean Anderson, Wake Forest University – DEAC Support
- NSF Grants DMR-1940324 and DMR-2242959

WAKE FOREST UNIVERSITY

NSF

HPC DEAC

Talk Outline

1. Background Information – Why study solid-state electrolytes?
2. Theory I – Detail some of the physics behind our research
3. Project I – What we learned about the (thio) boracite materials
4. Limitations we found attempting to continue (thio) boracite study
4. Theory II – Machine learning approach to extend first principles
5. Project II – Assessment of Allegro MLIP architecture using test system
6. Project III – Using Allegro to continue study of (thio) boracites
7. Conclusions
8. Questions

Lithium-Ion Batteries

- First mass production by Sony in 1991
- Widespread adoption in consumer electronics, electric vehicles, etc.
- Demand for lithium-ion Batteries has doubled in just 3 years
- >75% of current demand is electric vehicles

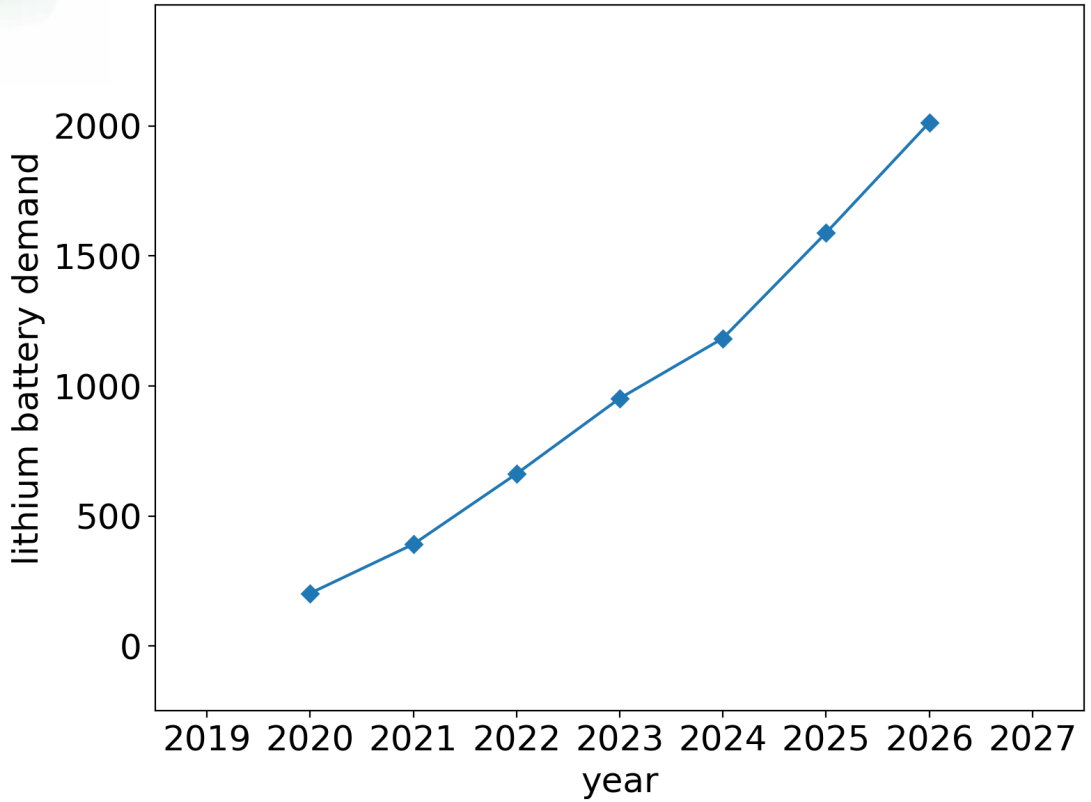

Conventional Lithium-Ion Batteries

- Lithium-ion batteries have 3 main components:
  - Anode (lithium-ion source)
  - Cathode (lithium-ion collector)
  - Electrolyte (connects anode and cathode)
- Anode and cathode provide voltage across the cell
- Electrolyte facilitates ion movement across the cell during charge/discharge
- Electrolyte is typically a liquid or gel
- Electric vehicle applications expose limitations with energy density, fast charging, safety, and lifespan

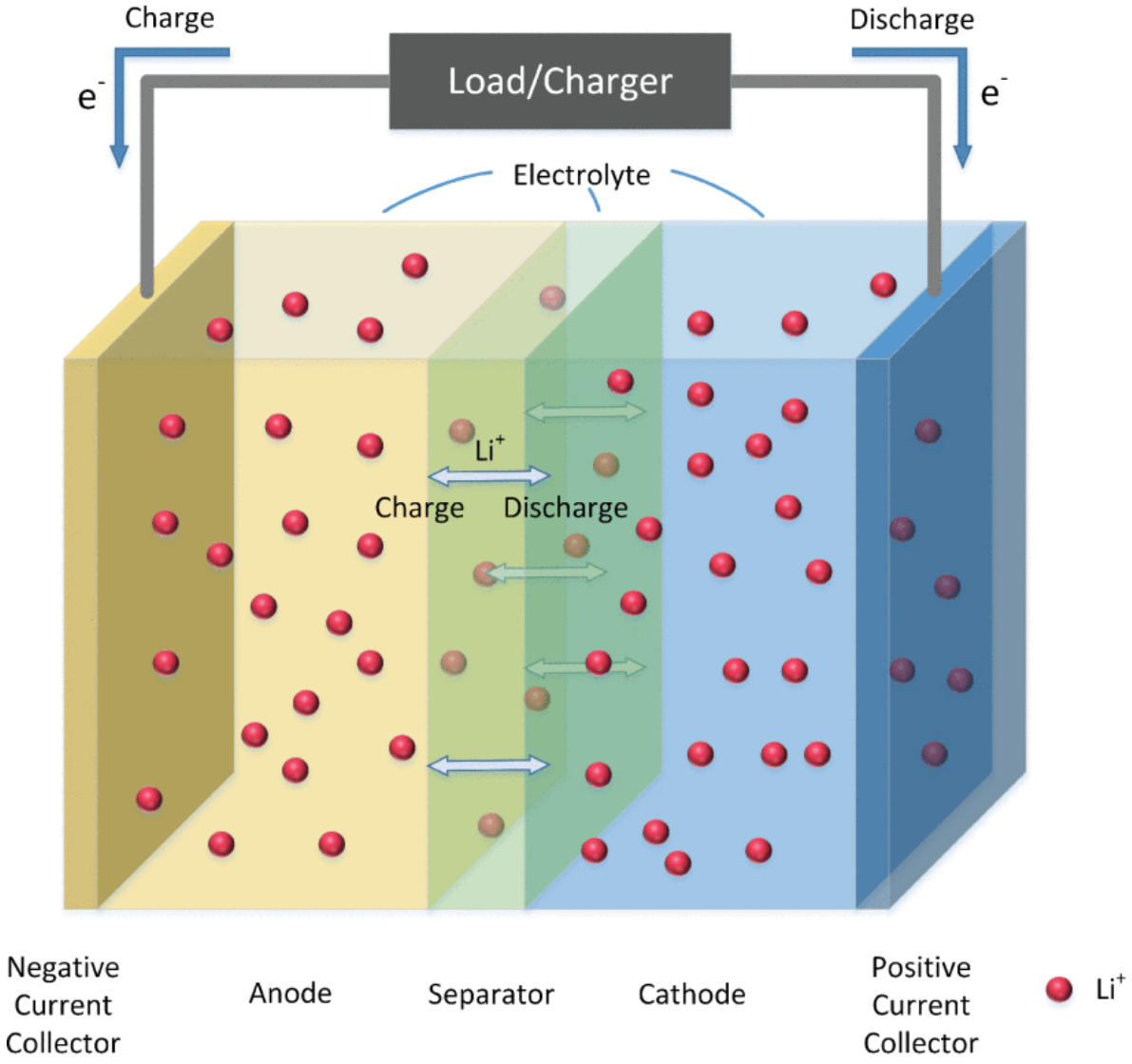

Solid-State Batteries

- Replaces liquid or gel electrolyte with a solid electrolyte material
- Ideal battery has pure lithium anode, decreasing weight and volume
- Promises higher energy density, faster charging, better safety and recyclability
- LiPON thin film cell developed at Oak Ridge in the 1990s, has scaling and cost limitations
- Kamaya et al (2011): studied solid electrolyte with higher ionic conductivity than liquids
- Current research designs have issues with lithium dendrite formation
- Solid-electrolyte research is essential
- Publications have doubled in 4 years, showing increased scientific interest

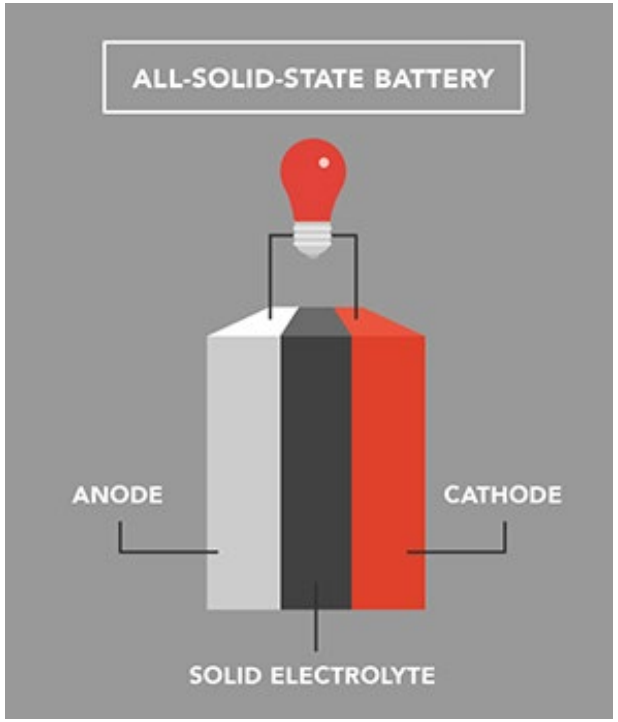

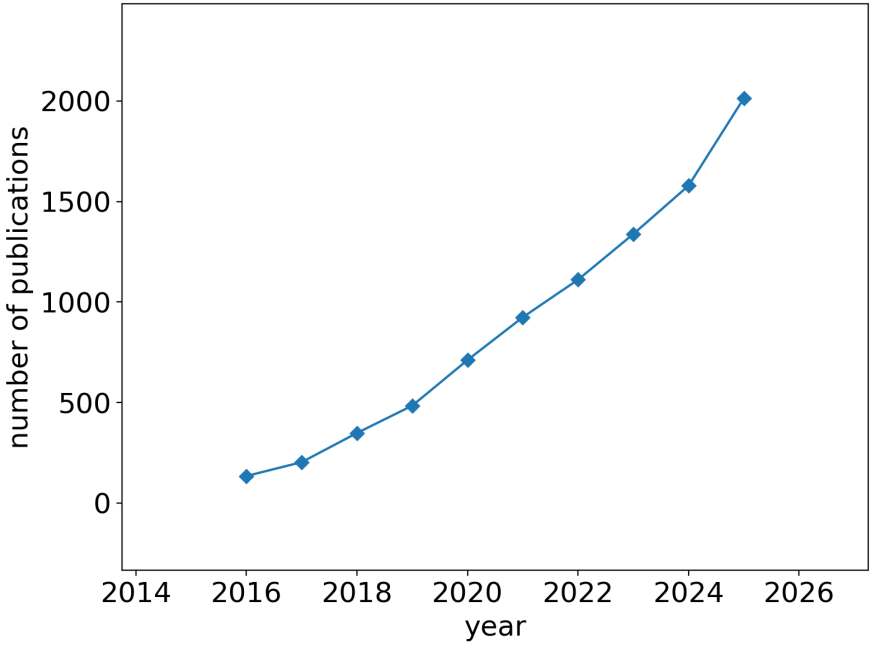

Computational Physics Theory I

- Crystaline materials can be modeled in a lattice unit cell
- Unit cells have lattice parameters and special symmetry sites
- Primitive cell is the smallest repeating subdivision of the crystal
- Symmetry sites determined by the space group of the lattice
- Sites can be fully or partially (fractionally) occupied

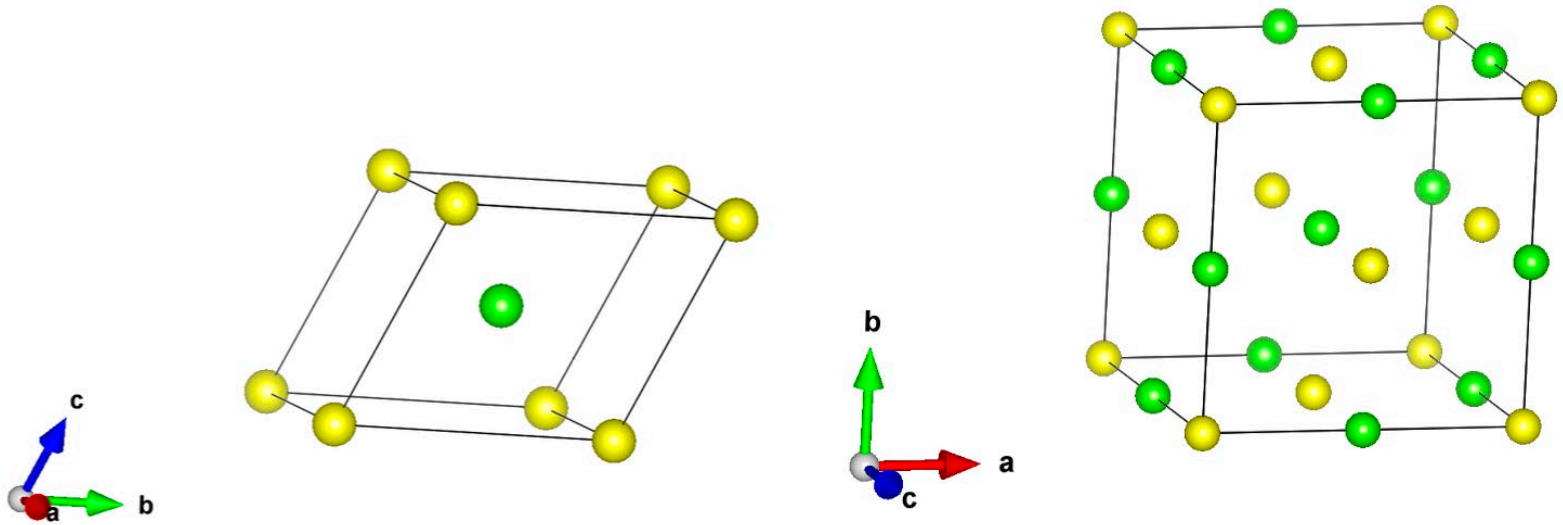

$NaCl$ primitive cell (left) and conventional cell (right)

Computational Physics Theory II

- Structural relaxation calculations minimize static lattice energy U_{SL}
- U_{SL} is from the electrostatic interactions within the material at 0K
- Equilibrium structure is found when U_{SL} is minimized (net force is zero)
- May distort, change volume, or lose structural symmetry
- Compare static lattice energies to find lower energy (preferred) structures
- U_{SL} is found by solving Kohn-Sham equations iteratively

$$E_{KS} = T_S[n] + \int d\mathbf{r} V_{\text{ext}}(\mathbf{r}) n(\mathbf{r}) + E_{\text{Hartree}} + E_{NN} + E_{xc}[n]$$

$$\left(H_{\text{KS}}^{\sigma} - \epsilon_i^{\sigma}\right) \phi_i^{\sigma} = 0$$

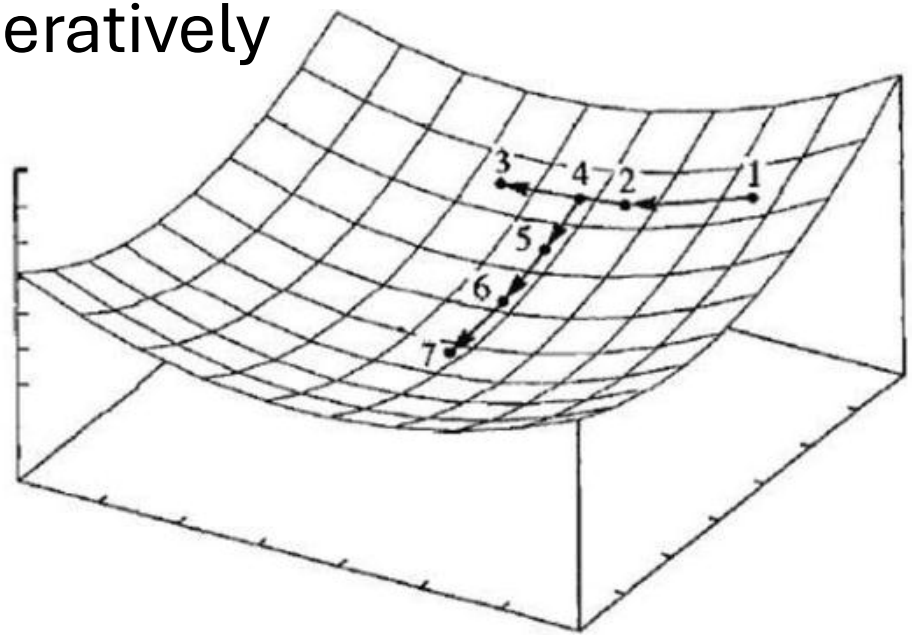

Computational Physics Theory III

- Phonons are quasiparticles representing vibrational modes in a crystal
- Finite differences treats displacements classically, solves for frequencies ω
- Frequencies are found as functions of the wave vector $\vec{\boldsymbol{k}}$ for an atomic site i
- These are calculated along a specific symmetry path through the lattice
- Can integrate the resultant dispersion curves to get PDOS and free energy

$$\det\left|\frac{1}{\sqrt{M_s M_{s'}}}C_{s,\alpha,s',\alpha'}(\mathbf{k})-\omega_{i,\mathbf{k}}^2\right|=0 \qquad C_{s,\alpha,s',\alpha'}(\mathbf{k})=\sum_{\mathbf{T}_n}e^{i\mathbf{k}\cdot\mathbf{T}_n}\frac{\partial^2 E(\mathbf{R})}{\partial\mathbf{R}_{s,\alpha}(0)\partial\mathbf{R}_{s',\alpha'}(\mathbf{T}_n)}=\frac{\partial^2 E(\mathbf{R})}{\partial\mathbf{u}_{s,\alpha}(\mathbf{k})\partial\mathbf{u}_{s'\alpha'}(\mathbf{k})}$$

$$F=U_{SL}+\frac{1}{2}\sum_{\mathbf{k},n}\hbar\omega_{\mathbf{k},n}+k_BT\sum_{\mathbf{k},n}\ln\left[1-e^{(-\hbar\omega_{\mathbf{k},n}/k_BT)}\right]$$

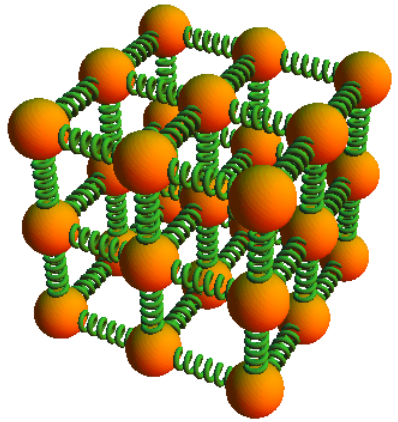

Computational Physics Theory IV

- First principles molecular dynamics give ionic trajectories over time
- Born-Oppenheimer approximation: nuclei are treated classically
- Can numerically integrate newton's equations for the nuclei
- After each integration step, electronic configuration is calculated using DFT
- From ensemble average of trajectories, we can estimate ionic conductivity
- Full conductivity is noisy: requires large number of ensembles
- Can use tracer approximation if ions are uncorrelated

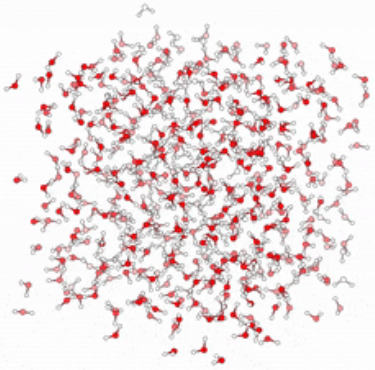

$$r(t+\Delta t) \approx 2r(t) - r(t-\Delta t) + \frac{F(t)}{m}(\Delta t)^2$$

$$\sigma^{\text{full}} = \frac{q_D^2}{6k_BT\Omega} \lim_{\tau\to\infty} \frac{1}{\tau} \left\langle \left| \sum_{i\in D} \mathbf{r}_i(\tau) - \mathbf{r}_i(0) \right|^2 \right\rangle \quad \sigma^{\text{tr}} = \frac{q_D^2}{6k_BT\Omega} \lim_{\tau\to\infty} \frac{1}{\tau} \left\langle \sum_{i\in D} |\mathbf{r}_i(\tau) - \mathbf{r}_i(0)|^2 \right\rangle$$

Project I

Computational investigation of the structural and electrolyte properties of the extended family of lithium (thio)boracite materials: $Li_4B_7O_{12}Cl$ and beyond

D. Cory Lynch,[1,*] Yan Li,[2,*] Pieremanuele Canepa,[2,3,4] and N. A. W. Holzwarth[5]

[1]*Department of Physics, Wake Forest University, Winston-Salem, North Carolina 27109, USA*

[2]*Department of Materials Science and Engineering, National University of Singapore, Singapore 119077, Singapore*

[3]*Department of Electrical and Computer Engineering, University of Houston, Houston, Texas 77204, USA*

[4]*Texas Center for Superconductivity at the University of Houston (TcSUH), Houston, Texas 77204, USA*

[5]*Department of Physics, Wake Forest University, Winston-Salem, North Carolina 27109, USA*

(Received 13 December 2023; revised 5 March 2024; accepted 15 May 2024; published 3 June 2024)

Motivated by previous investigations that showed very promising high ionic conductivities within relatively stable framework structures, we report a systematic first-principles study of the extended family of lithium (thio)boracites, consisting of eight chemical compositions. Three of the compositions—$Li_4B_7O_{12}Cl$, $Li_4Al_3B_4O_{12}Cl$, and $Li_6B_7S_{13}Cl$—are comparable to synthesized and analyzed materials reported in the experimental literature. The five additional compositions—$Li_4B_7S_{12}Cl$, $Li_4Al_3B_4S_{12}Cl$, $Li_6B_7O_{13}Cl$, $Li_6Al_3B_4O_{13}Cl$, and $Li_6Al_3B_4S_{13}Cl$—are predicted from the computational modeling and analysis presented in this paper. For each material, idealized ordered rhombohedral, cubic, or monoclinic ground-state structures are determined.

Project I Motivation: (Thio)Boracite Motivation

- 3 experimentally synthesized and studied materials:
  - $Li_4B_7O_{12}Cl$ Jeitschko et al, 1977. DOI: 10.1107/S0567740877009443
  - $Li_4Al_3B_4O_{12}Cl$ Kajihara et al, 2017. DOI: 10.1246/bcsj.20170242
  - $Li_6B_7S_{13}Cl$ Kaup et al, 2021. DOI: 10.1021/jacs.1c00941
- All have cubic $F\bar{4}3c$ structure with fractionally occupied lithium sites
- $Li_6B_7S_{13}Cl$ has dynamically unstable tetragonal polymorph
- Previous work by Dr. Li and Dr. Holzwarth on $Li_4B_7O_{12}Cl$

  2022. DOI: 10.1103/PhysRevMaterials.6.045403
- Space of chemical composition not experimentally studied
  - $O \leftrightarrow S$ substitutions
  - $B \rightarrow Al$ partial substitutions
  - Addition of Li_2X ($X = O, S$), i.e., $Li_4B_7O_{12}Cl + Li_2O \rightarrow Li_6B_7O_{13}Cl$

Project I Motivation: Previous $Li_4B_7O_{12}Cl$ Study

- Experiment: "Disordered" cubic $F\bar{4}3c$ structure with fractional Li occupancy
- Can define "ordered" cubic $F\bar{4}3c$ structure with fully occupied lithium sites
- New slightly distorted rhombohedral $R3c$ structure found with lower static lattice energy
- Partially occupied lithium sites in $F\bar{4}3c$ map to fully occupied sites in $R3c$
- "Natural" interstitial sites in void region facilitate lithium-ion diffusion through the material

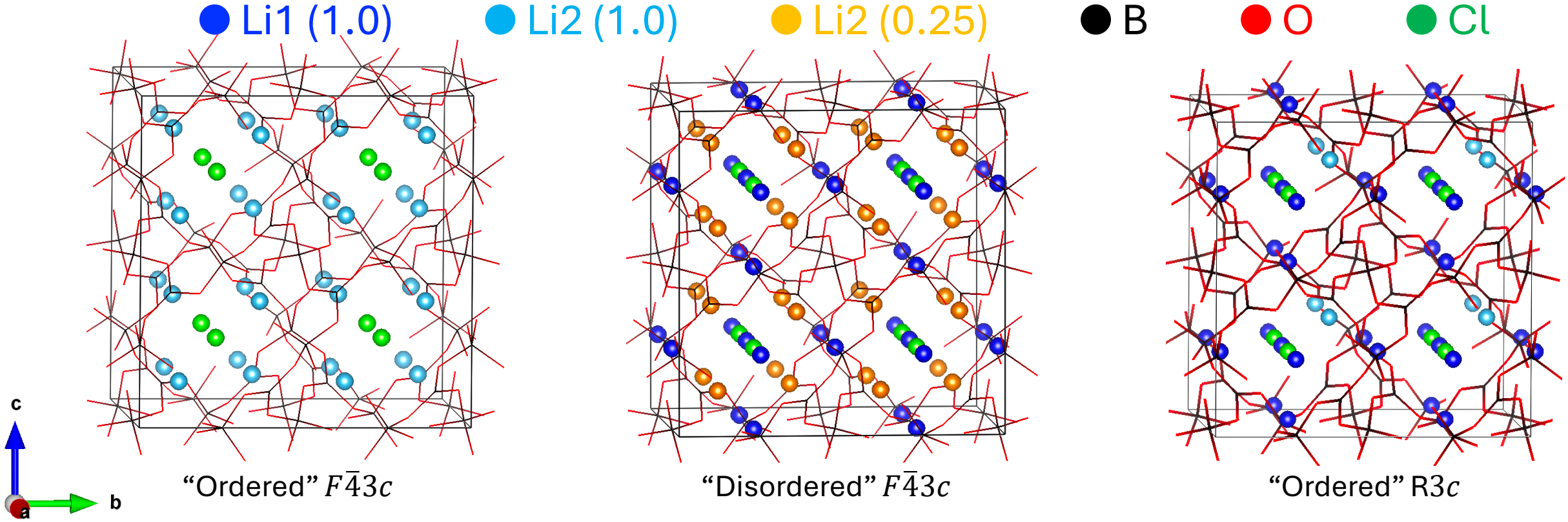

"Ordered" $F\bar{4}3c$ "Disordered" $F\bar{4}3c$ "Ordered" R3c

Project I (Thio) Boracite Study: Li_4 Materials

- Previously studied $Li_4B_7O_{12}Cl$ (based on experimental material)
- Newly investigated $Li_4Al_3B_4O_{12}Cl$ (based on experimental material)
- Newly predicted substitutions: $Li_4B_7S_{12}Cl$ and $Li_4Al_3B_4S_{12}Cl$
- All have lower energy $R3c$ structures except $Li_4B_7S_{12}Cl$ ($F\bar{4}3c$)

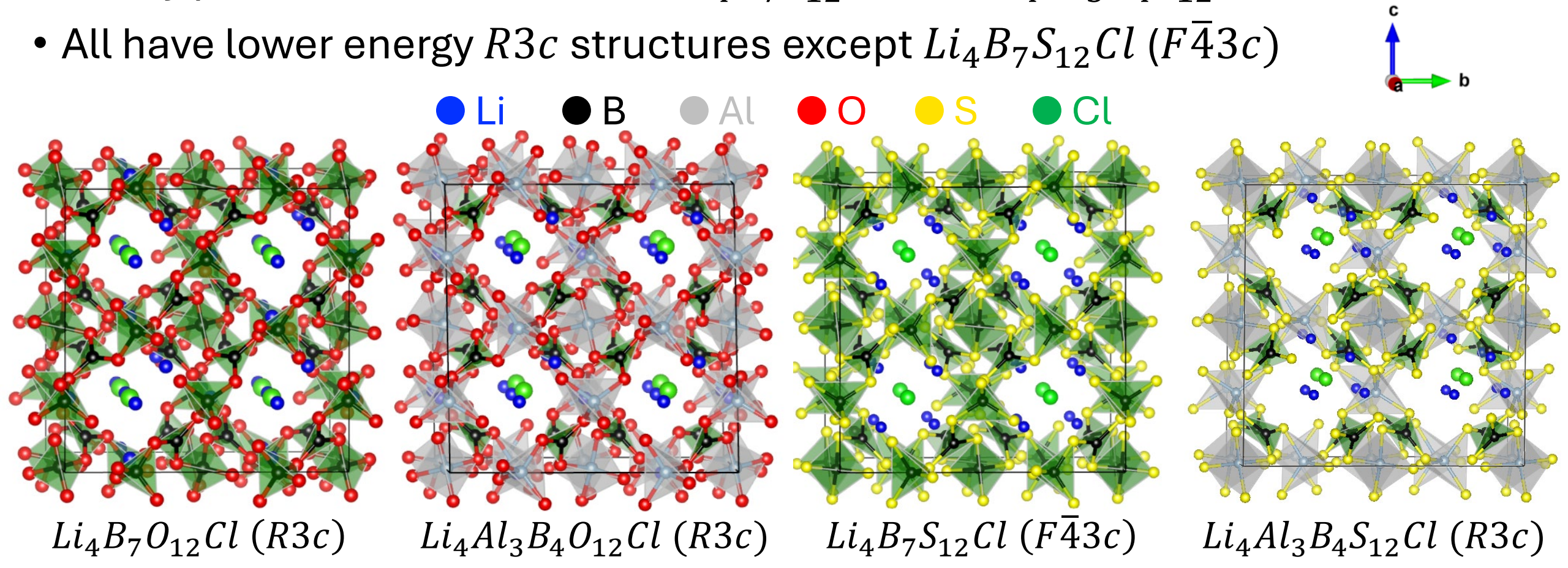

Project I (Thio) Boracite Study: New Cc Structure

- Lithium thioboracite $Li_6B_7S_{13}Cl$
- Kaup et al synthesized and studied related material $Li_6B_7S_{13}I$
- We chose to use Cl as the halogen instead of I
- They found a cubic $F\bar{4}3c$ structure with partial occupancy of the Li sites
- Only has tetragonal BS_4 units in framework
- Additionally found a tetragonal $I\bar{4}c2$ polymorph
- This was found to be be dynamically unstable
- We verified the $I\bar{4}c2$ polymorph to be dynamically unstable for the Cl variant as well
- Our investigations found a new lower energy monoclinic Cc structure for the Cl variant

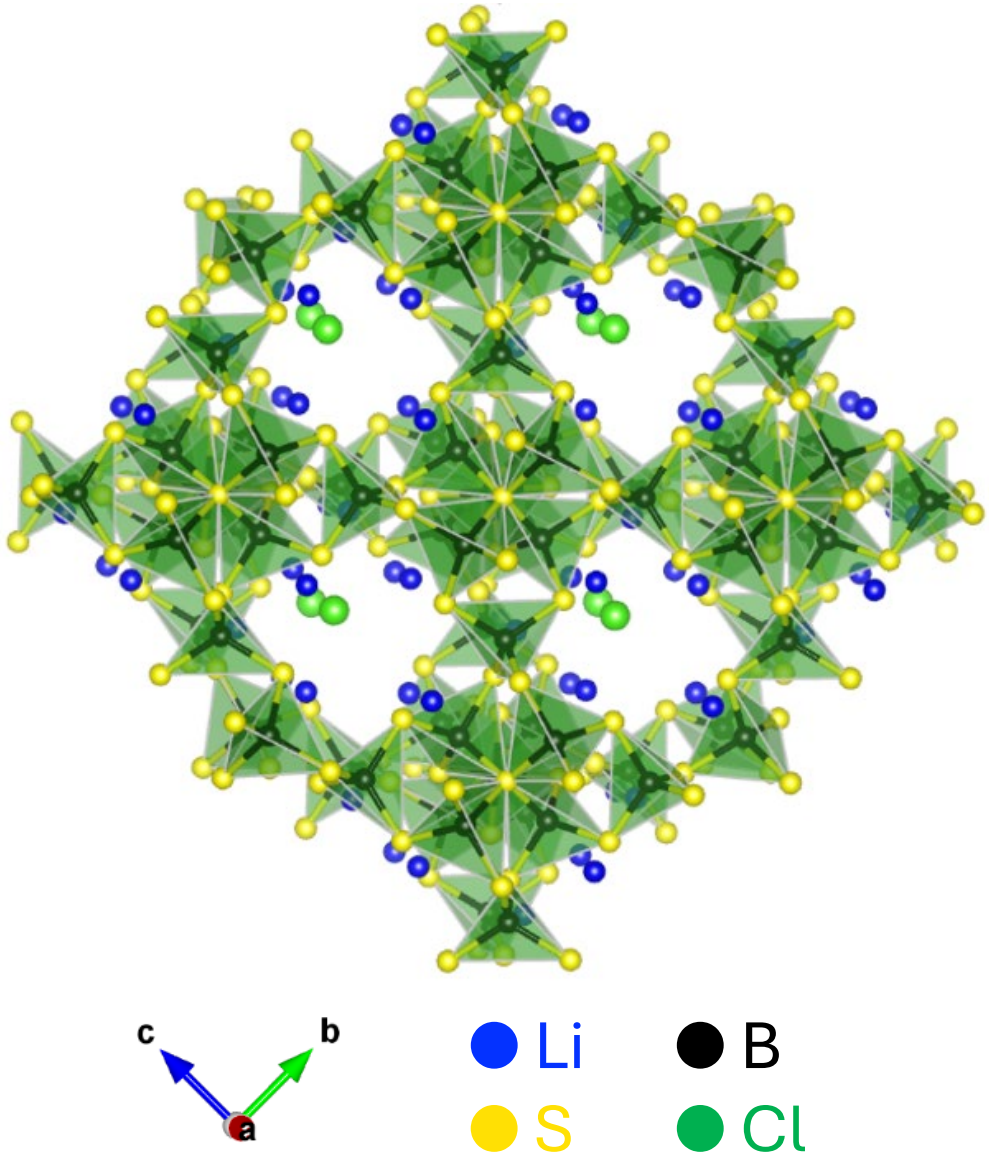

Project I (Thio) Boracite Study: Li_6 Materials

- Newly investigated $Li_6B_7S_{13}Cl$ (based on experimental material with I)
- Newly predicted substitutions: $Li_6B_7O_{13}Cl$, $Li_6Al_3B_4O_{13}Cl$, $Li_6Al_3B_4S_{13}Cl$
- All have lower energy Cc structures except $Li_6B_7O_{13}Cl$ $(R3c)$

Li B Al O S Cl

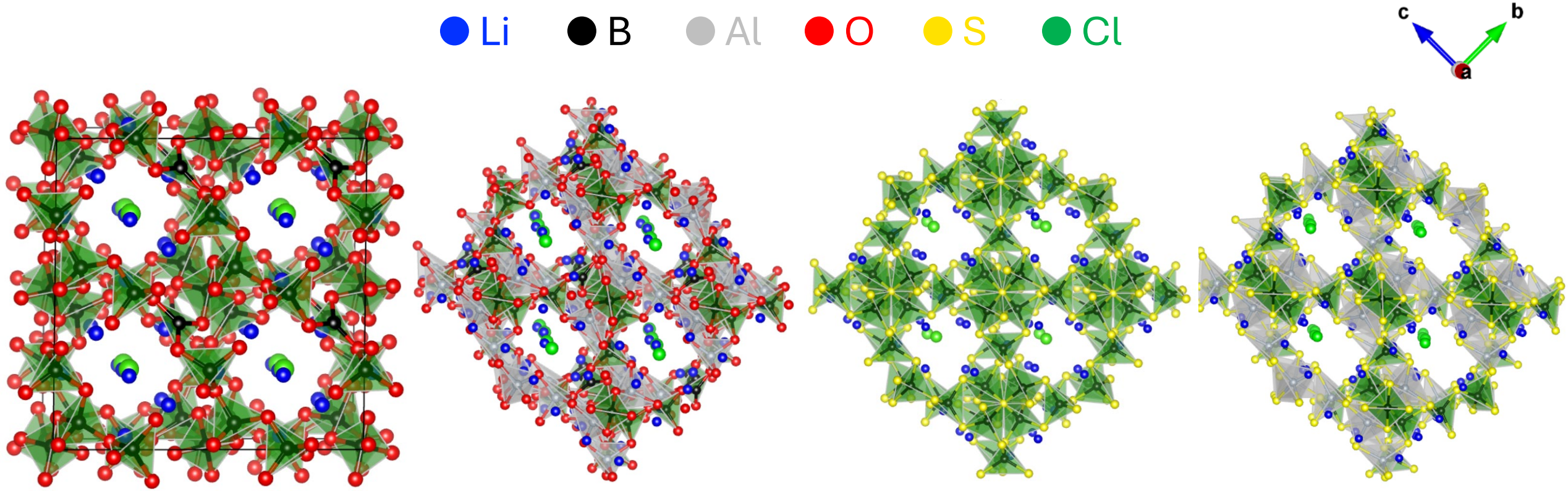

$Li_6B_7O_{13}Cl$ $(R3c)$ $Li_6Al_3B_4O_{13}Cl(Cc)$ $Li_6B_7S_{13}Cl(Cc)$ $Li_6Al_3B_4S_{13}Cl(Cc)$

Project I (Thio) Boracite Study: Structural Results

Formula	SG	Lattice	Angle	Tri/Tet	Vol	ΔU_{SL}
$Li_4B_7O_{12}Cl$	$R3c$	$a = 12.1$ (12.1410)[a]	$\alpha = 90.1$ (90.0)[a]	4/3	223.0	0.00
$Li_4B_7O_{12}Cl$	$F\bar{4}3c$	$a = 12.2$	$\alpha = 90.0$	4/3	224.8	0.21
$Li_6B_7O_{13}Cl$	$R3c$	$a = 12.2$	$\alpha = 89.4$	1/6	224.3	–1.58
$Li_6B_7O_{13}Cl$	Cc	$a = 15.0$	$\alpha = 90.0$	1/6	225.8	–1.26
		$b = 8.6$	$\beta = 124.7$			
		$c = 8.6$	$\gamma = 90.0$			
$Li_4Al_3B_4O_{12}Cl$	$R3c$	$a = 13.0$ (12.9687)[b]	$\alpha = 91.1$ (90.0)[b]	4/3	275.6	0.00
$Li_4Al_3B_4O_{12}Cl$	$F\bar{4}3c$	$a = 13.0$	$\alpha = 90.0$	4/3	272.0	1.19
$Li_6Al_3B_4O_{13}Cl$	$R3c$	$a = 13.0$	$\alpha = 88.3$	1/6	275.0	–0.22
$Li_6Al_3B_4O_{13}Cl$	Cc	$a = 16.0$	$\alpha = 90.0$	1/6	273.8	–0.40
		$b = 8.9$	$\beta = 127.1$			
		$c = 9.7$	$\gamma = 90.0$			
$Li_4B_7S_{12}Cl$	$R3c$	$a = 14.9$	$\alpha = 89.8$	4/3	415.7	0.00
$Li_4B_7S_{12}Cl$	$F\bar{4}3c$	$a = 14.9$	$\alpha = 90.0$	4/3	414.6	–0.05
$Li_6B_7S_{13}Cl$	$R3c$	$a = 15.1$ (15.245)[c]	$\alpha = 89.2$ (90.0)[c]	0/7	431.3	–0.96
$Li_6B_7S_{13}Cl$	Cc	$a = 18.5$	$\alpha = 90.0$	0/7	429.9	–1.05
		$b = 10.5$	$\beta = 124.6$			
		$c = 10.8$	$\gamma = 90.0$			
$Li_4Al_3B_4S_{12}Cl$	$R3c$	$a = 16.1$	$\alpha = 89.6$	4/3	516.9	0.00
$Li_4Al_3B_4S_{12}Cl$	$F\bar{4}3c$	$a = 15.8$	$\alpha = 90.0$	4/3	489.0	0.85
$Li_6Al_3B_4S_{13}Cl$	$R3c$	$a = 16.1$	$\alpha = 87.8$	0/7	519.7	–0.34
$Li_6Al_3B_4S_{13}Cl$	Cc	$a = 19.8$	$\alpha = 90.0$	0/7	508.2	–0.65
		$b = 10.8$	$\beta = 126.1$			
		$c = 11.8$	$\gamma = 90.0$			

Project I (Thio) Boracite Study: Phonon Analysis

- Phonon dispersion plots and PDOS calculated for all materials
- Here we see dispersion + PDOS plots for the lowest energy structures of the three materials investigated based on experimental compounds
- Lowest energy structures of all 8 materials have real ω→ dynamic stability

$Li_4B_7O_{12}Cl\ (R3c)$

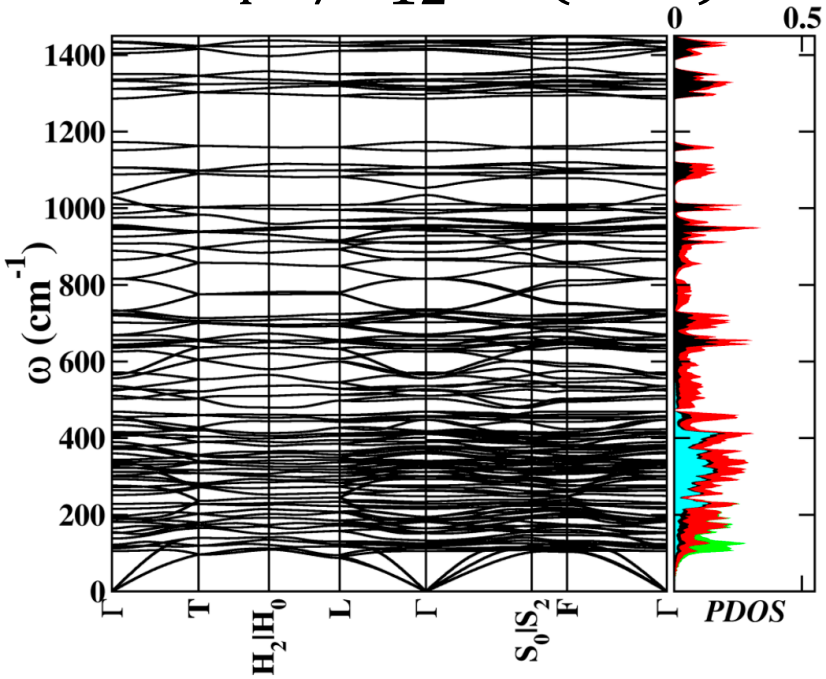

$Li_4Al_3B_4O_{12}Cl\ (R3c)$

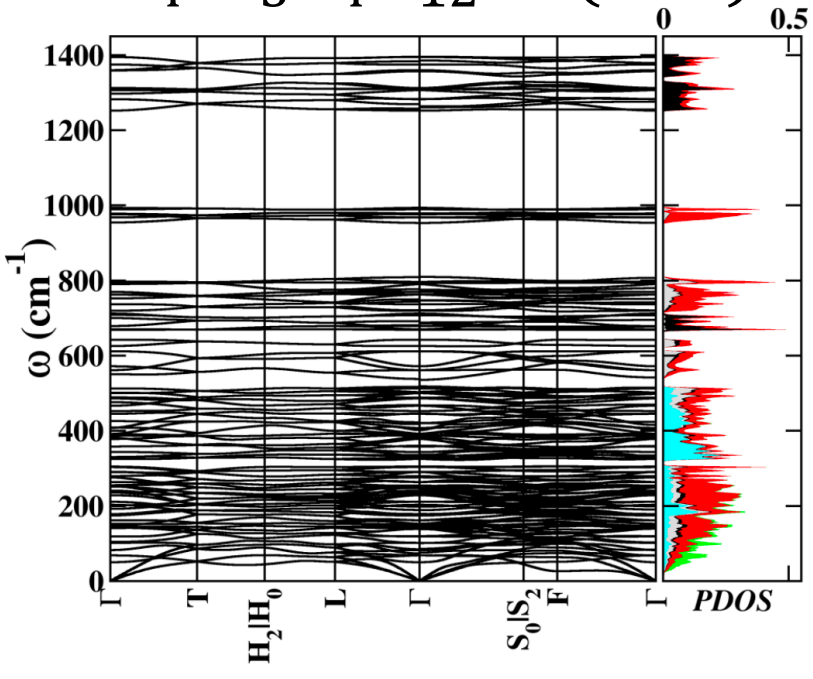

$Li_6B_7S_{13}Cl\ (Cc)$

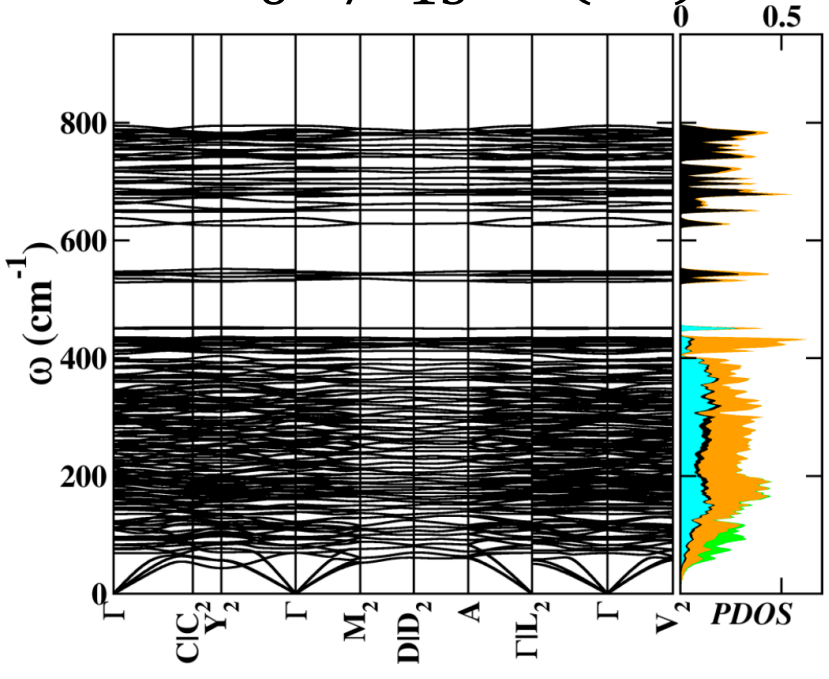

Project I (Thio) Boracite Study: Free Energy

- The free energy of the materials can be calculated from the PDOS
- Free energy is a function of temperature, is a rough estimate of stability (static lattice + vibrations)
- Here we see the same patterns that were present from SL energies
- Li_6 materials are energetically favorable vs. Li_4 materials
- Li_4 materials generally favor $R3c$
- Exception is $Li_4B_7S_{12}Cl$ $(F\bar{4}3c)$
- Li_4 materials favor generally Cc
- Exception is $Li_6B_7O_{13}Cl$ $(R3c)$

Formula	SG	ΔF $T = 0$ K	ΔF $T = 300$ K	ΔF $T = 400$ K
$Li_4B_7O_{12}Cl$	$R3c$	0.00	0.00	0.00
$Li_6B_7O_{13}Cl$	$R3c$	−1.59	−1.53	−1.50
$Li_6B_7O_{13}Cl$	Cc	−1.27	−1.22	−1.20
$Li_4Al_3B_4O_{12}Cl$	$R3c$	0.00	0.00	0.00
$Li_6Al_3B_4O_{13}Cl$	$R3c$	−0.25	−0.20	−0.18
$Li_6Al_3B_4O_{13}Cl$	Cc	−0.42	−0.35	−0.32
$Li_4B_7S_{12}Cl$	$R3c$	0.00	0.00	0.00
$Li_4B_7S_{12}Cl$	$F\bar{4}3c$	−0.07	−0.09	−0.10
$Li_6B_7S_{13}Cl$	$R3c$	−0.96	−0.92	−0.89
$Li_6B_7S_{13}Cl$	Cc	−1.05	−0.99	−0.96
$Li_4Al_3B_4S_{12}Cl$	$R3c$	0.00	0.00	0.00
$Li_6Al_3B_4S_{13}Cl$	$R3c$	−0.33	−0.23	−0.19
$Li_6Al_3B_4S_{13}Cl$	Cc	−0.63	−0.52	−0.47

Project I (Thio) Boracite Study: Summary

- 3 experimentally investigated (thio)boracite materials as motivation:

  $Li_4B_7O_{12}Cl$ $Li_4Al_3B_4O_{12}Cl$ $Li_6B_7S_{13}I$
- Previous $Li_4B_7O_{12}Cl$ studies found lower energy $R3c$ distortion
- This work found:
- Similar lower energy $R3c$ distortion for $Li_4Al_3B_4O_{12}Cl$
- New lower energy Cc structure for $Li_6B_7S_{13}Cl$
- Substitutions yield computationally predicted materials:
- $Li_4B_7S_{12}Cl$ ($F\bar{4}3c$) and $Li_4Al_3B_4S_{12}Cl$ ($R3c$)
- $Li_6B_7O_{13}Cl$ ($R3c$), $Li_6Al_3B_4O_{13}Cl$ (Cc), and $Li_6Al_3B_4S_{13}Cl$ (Cc)
- All materials are predicted to be dynamically stable
- Convex hull and voltage window analysis assessed chemical stability

(Thio) Boracite Continuation: Ionic Diffusion

$Li_4Al_3B_4O_{12}Cl$ $(R3c)$

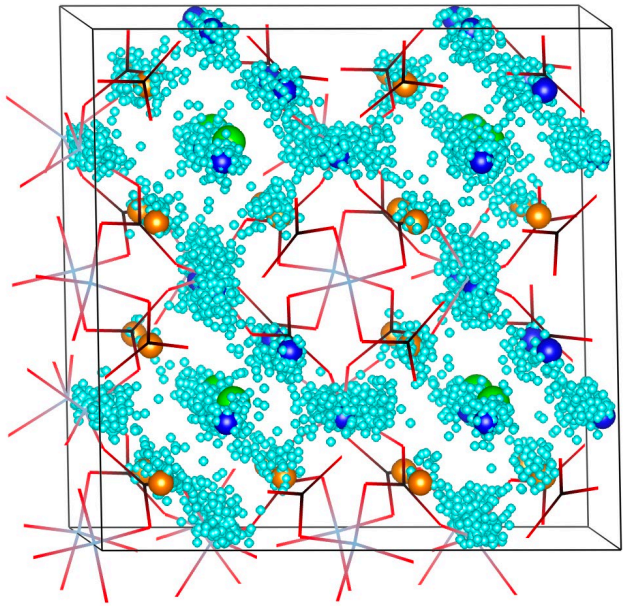

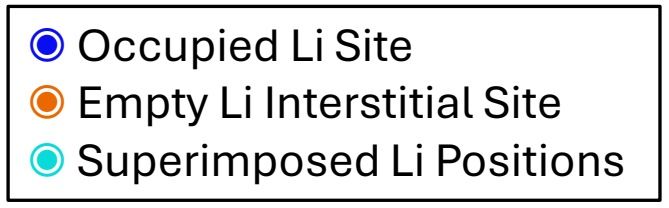

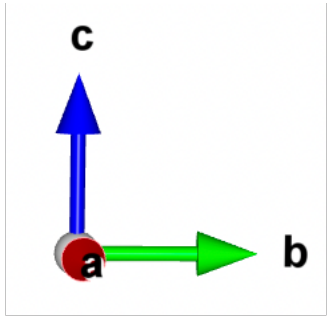

$Li_4Al_3B_4S_{12}Cl$ $(R3c)$

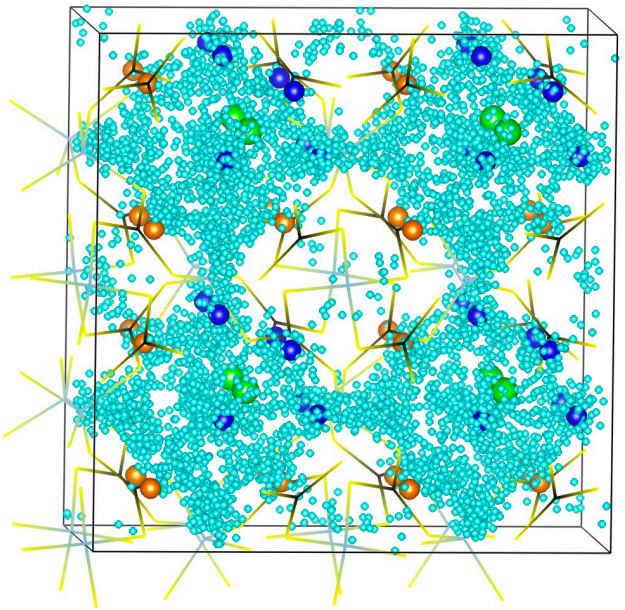

- Lithium superposition plots qualitatively hint at good ionic diffusion
- Li positions superimposed over ~23 ps of simulation time
- Sampled every 50 timesteps at 1100K simulation temperature
- Large simulation cells and number of atoms result in computational roadblocks: first-principles methods can simulate only 0.12 ps per day

Machine Learned Interatomic Potentials I

- Machine learning is a data driven optimization method
- Neural networks are increasingly utilized in science
- Take a known sets of input and outputs (training data)
- Optimize a predictive function so that for each training example, the error between the predicted output and the known (correct) output is minimized
- This process “learns” the correct function to match the training data
- Validation set used as a measure of interpolative capability, is used to define the “best” model
- Important to choose “hyperparameters” (settings) wisely and to create high-quality training and validation datasets to provide sufficient input range

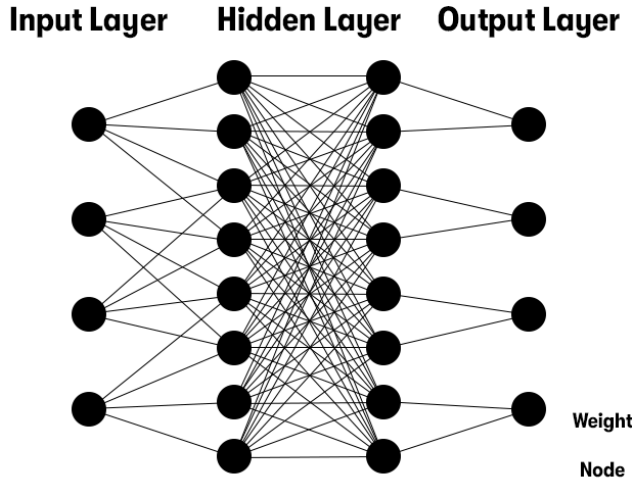

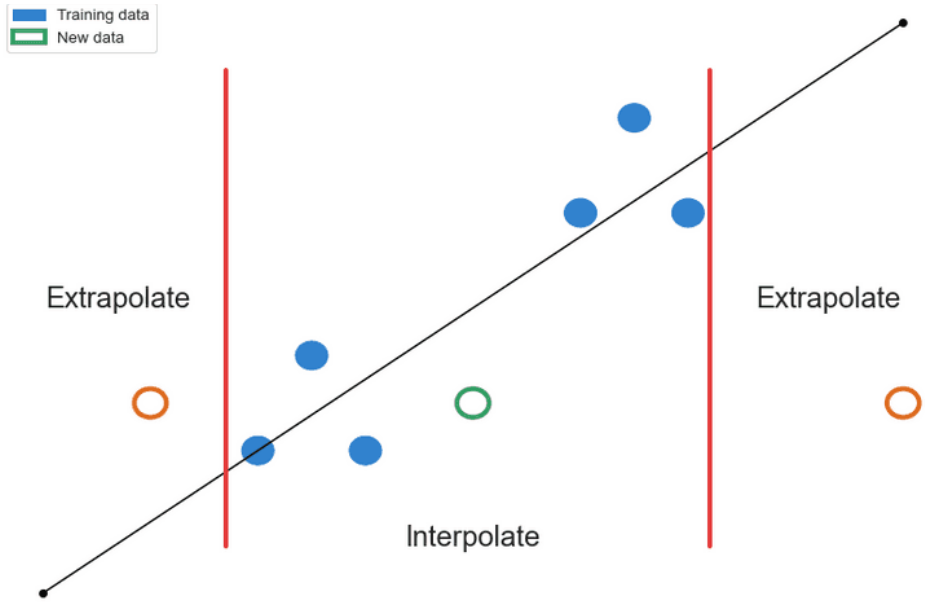

Machine Learned Interatomic Potentials II

- For machine learned interatomic potentials, it is important to construct neural networks with physical “representations” of atoms
- Nequip[1] is an atom-centered “message-passing” graph neural network
- Initial atomic “embedding” contains radial and spherical basis functions
- Message passing “layers” allow the atomic representations to then be “learned” by mixing neighboring atomic embeddings intelligently
- Predictive function outputs learned atomic energy for an atomic site i

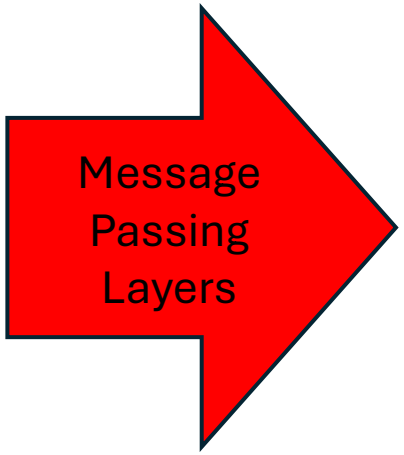

$$E_{\text{tot}} = \sum_{i=1}^{N} \sigma_{Z_i} E_i + \mu_{Z_i}$$

[1] Batzner, Musaelian et al, 2022. DOI: 10.1038/s41467-022-29939-5

Machine Learned Interatomic Potentials III

- Message passing graph networks have scaling problems by nature
- After each successive message passing step, information aggregates such that the effective radius of interaction increases
- Allegro[1] attempts to mitigate this with a strictly local graph network approach
- Utilizes a pair centered representation which forces interactions to be fixed within a radius r_{cut}
- Has similar accuracy to Nequip with greatly improved efficiency and scalability
- Predictive function outputs pair energies

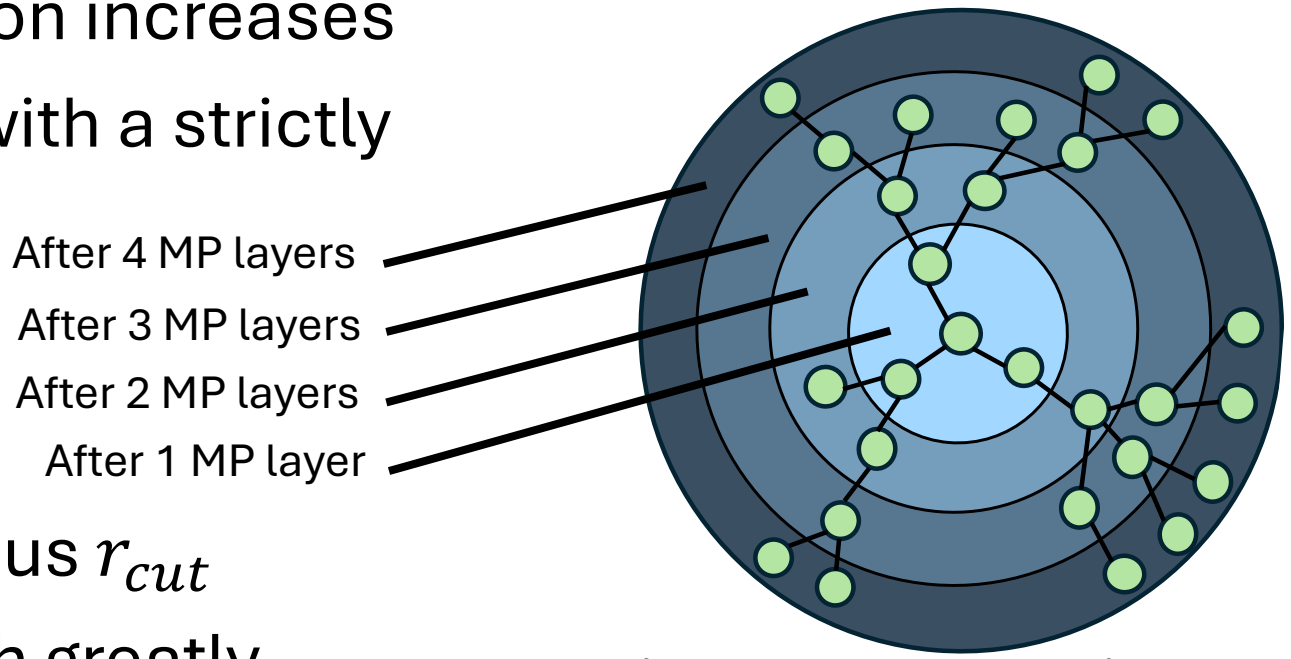

$$E_{\text{tot}} = \sum_{i=1}^{N} \sigma_{Z_i} \left(\sum_{j \in \mathcal{N}(i)} \sigma_{Z_i, Z_j} E_{ij} \right) + \mu_{Z_i}$$

[1] Musaelian, Batzner, et al, 2023. DOI: 10.1038/s41467-023-36329-y

Project II

PREPRINT MANUSCRIPT

A study of the use of machine learning methodology for computing ionic conductivity in an example solid state electrolyte material

D. Cory Lynch,[1] Chuin Wei Tan,[2] and N. A. W. Holzwarth[1]

[1] *Department of Physics, Wake Forest University, Winston-Salem, NC 27109, USA*
[2] *John A. Paulson School of Engineering and Applied Sciences, Harvard University, Cambridge, MA 02138, USA*

Realistically simulating macroscopic phenomena from the knowledge of atomic scale interactions has challenged generations of computational scientists. In the present paper, we examine how machine learning methods can be used towards accomplishing the "ensemble sampling" envisioned for evaluating the Green-Kubo formulation of the full ionic conductivity of a solid electrolyte system. This work explores some of the advantages and challenges of using Allegro machine learned interatomic potentials together with traditional computational algorithms toward the goal of finding ways in which it can best be used to enhance computational methodologies. Enhanced computational methodolgies can lead to advances in understanding of basic phenomena through more realistic simulations of materials and their properties. In particular, the computational efficiency and accuracy of the Allegro trained interatomic potentials opens the possibility of performing simulations that can more closely represent conditions of experimental measurements.

Project II Allegro Assessment: Test System

- Test system used for Allegro assessment based on study of $Li_3PO_4/\mathrm{Li}_4SiO_4$ by Deng et al[1]
- Loosely based on their disordered structural details
- Two structures considered with different Si sites
- Aptly named “S1” and “S2”

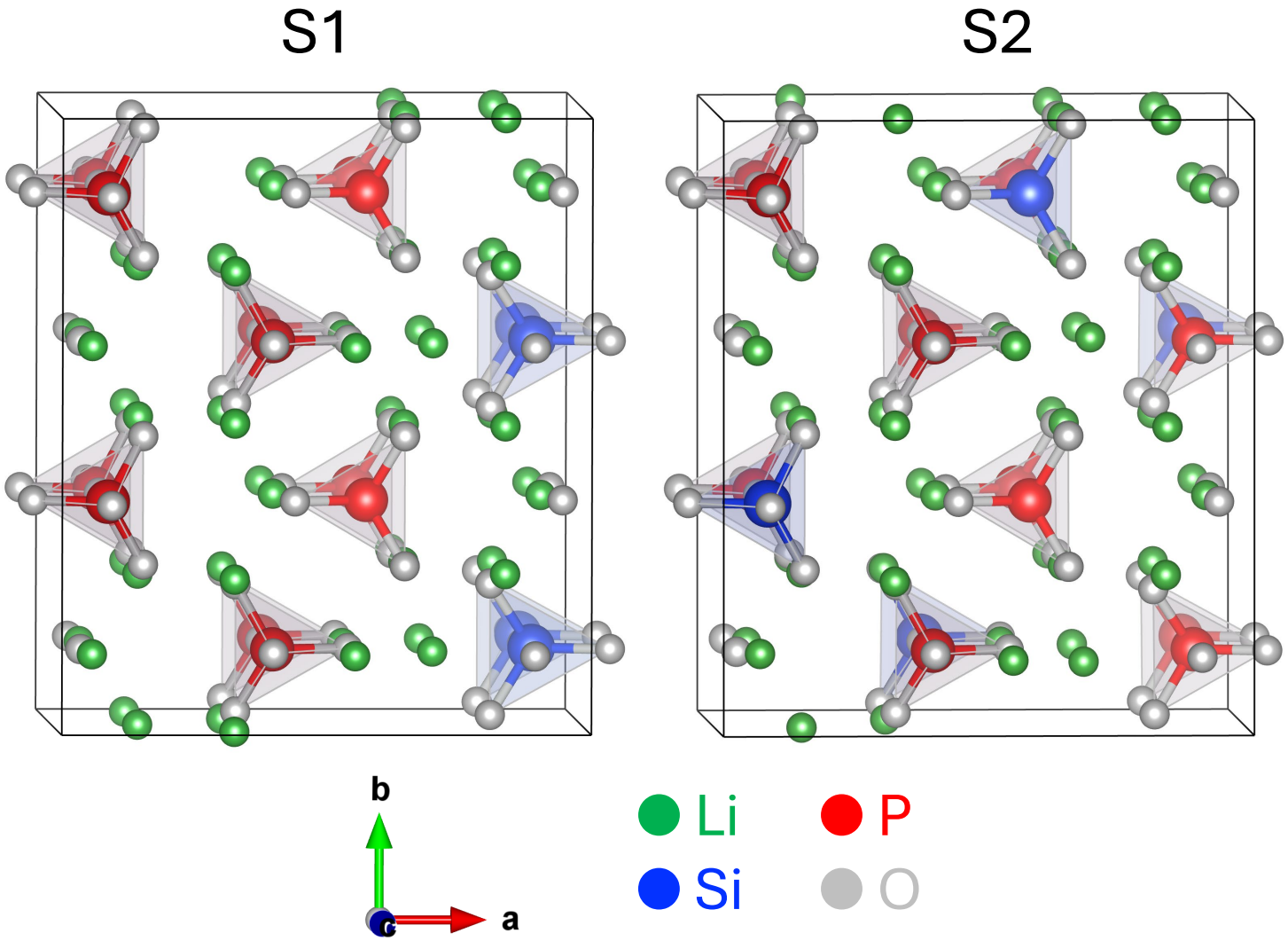

[1] Deng, et al, 2015. DOI: 10.1021/jacs.5b04444

Project II Allegro Assessment: Initial Testing I

- Before thorough testing can be done, we must familiarize ourselves with the software and determine optimal settings
- One important choice is dataset size
- Dataset size impacts trained model's interpolative capacity
- More "diverse" dataset yields better generalizability to similar structures encountered during MD simulations
- Training results seen here for 2500, 5000, and 7500 input dataset sizes with struct. S1
- Input datasets randomly split into training/validation datasets at 80:20 ratio
- 5000 structure input dataset most optimal

Avg. Energy/Atom Error vs. Dataset Size

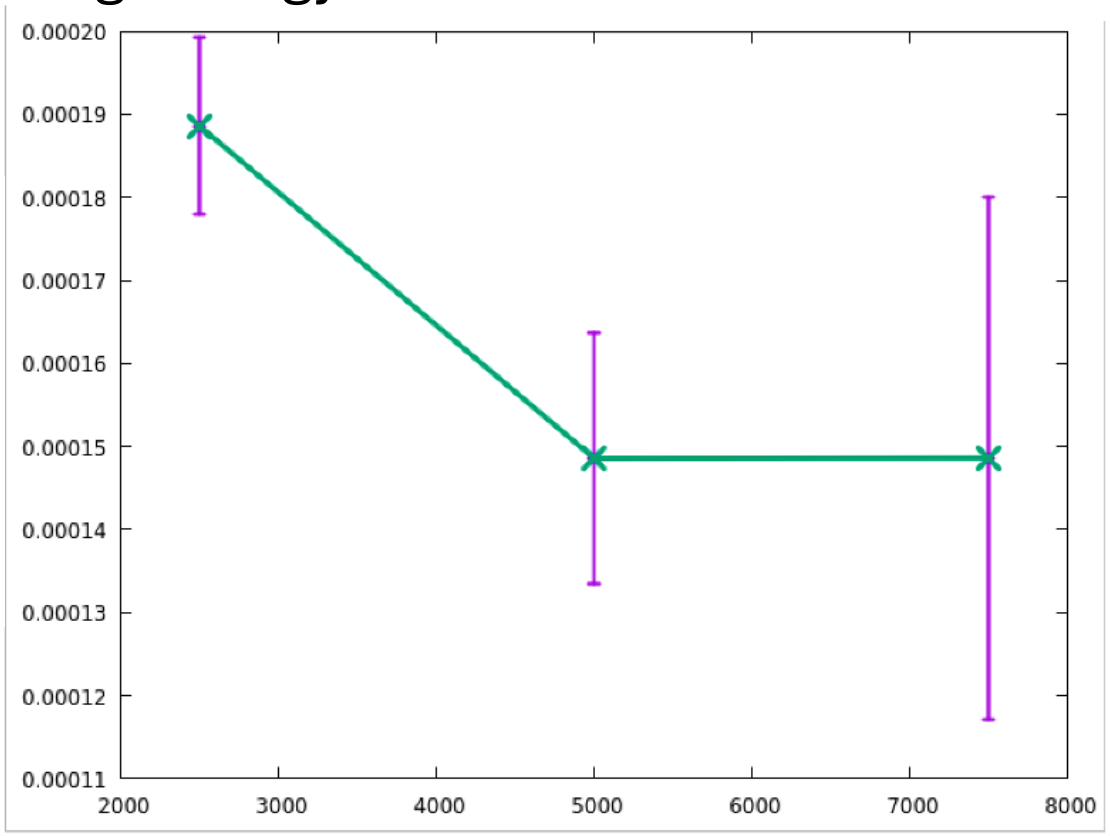

$$E^{D}_{\mathrm{MAE}} = \frac{1}{N_C}\sum_{\alpha=1}^{N_C}|\hat{E}_\alpha - E_\alpha|$$

Project II Allegro Assessment: Initial Testing II

- After determining optimal dataset size, we need to determine the hyperparameters to train our model with
- Perhaps most important is the choice of r_{cut} – pair interaction potential range
- Too short: Not enough pair interactions
- Too long: negligible contributions with large computational overhead
- In our short test of different r_{cut} values, we found 6.0 Å to be optimal for the test material (structure S1)

Avg. Energy/Atom Error vs. r_{cut} Choice

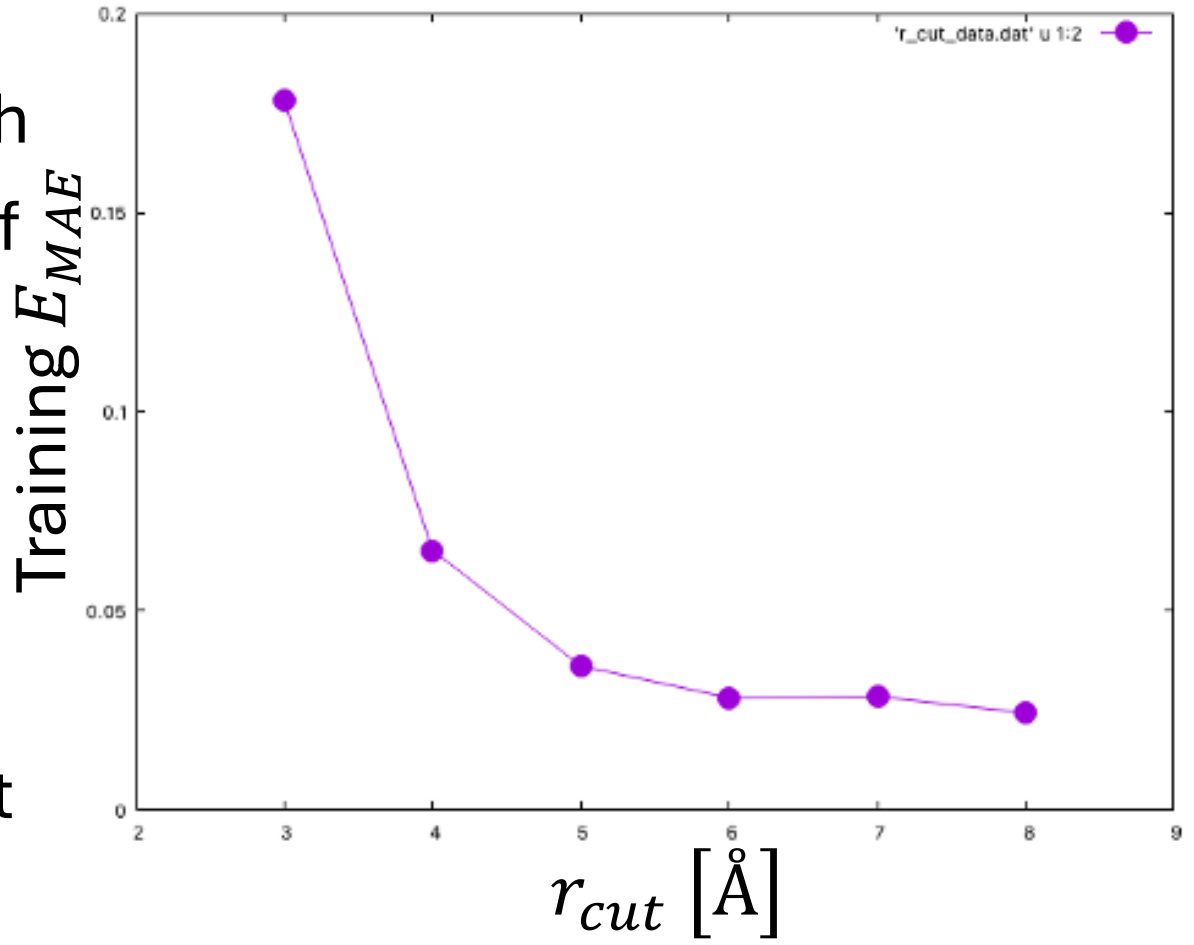

Project II Allegro Assessment: Initial Testing III

- In addition to r_{cut}, there are many other important hyperparameters to choose
- 4 found to be most impactful on error
- From preliminary testing, we selected 3 model "sizes" with parameters seen here
- Large adds minimal benefit over medium with huge increase in resource demand
- Small and medium found to be good candidates for further testing

	small	medium	large
r_{cut}	6.0	6.0	6.0
l_{max}	1	2	3
n_{tensor}	16	32	64
n_{scalar}	32	64	128
MLP_{dims}	1×32	2×64	3×128
n_{params}	25K	91K	387K

Avg. Energy/Atom Error vs. Hyper Choice

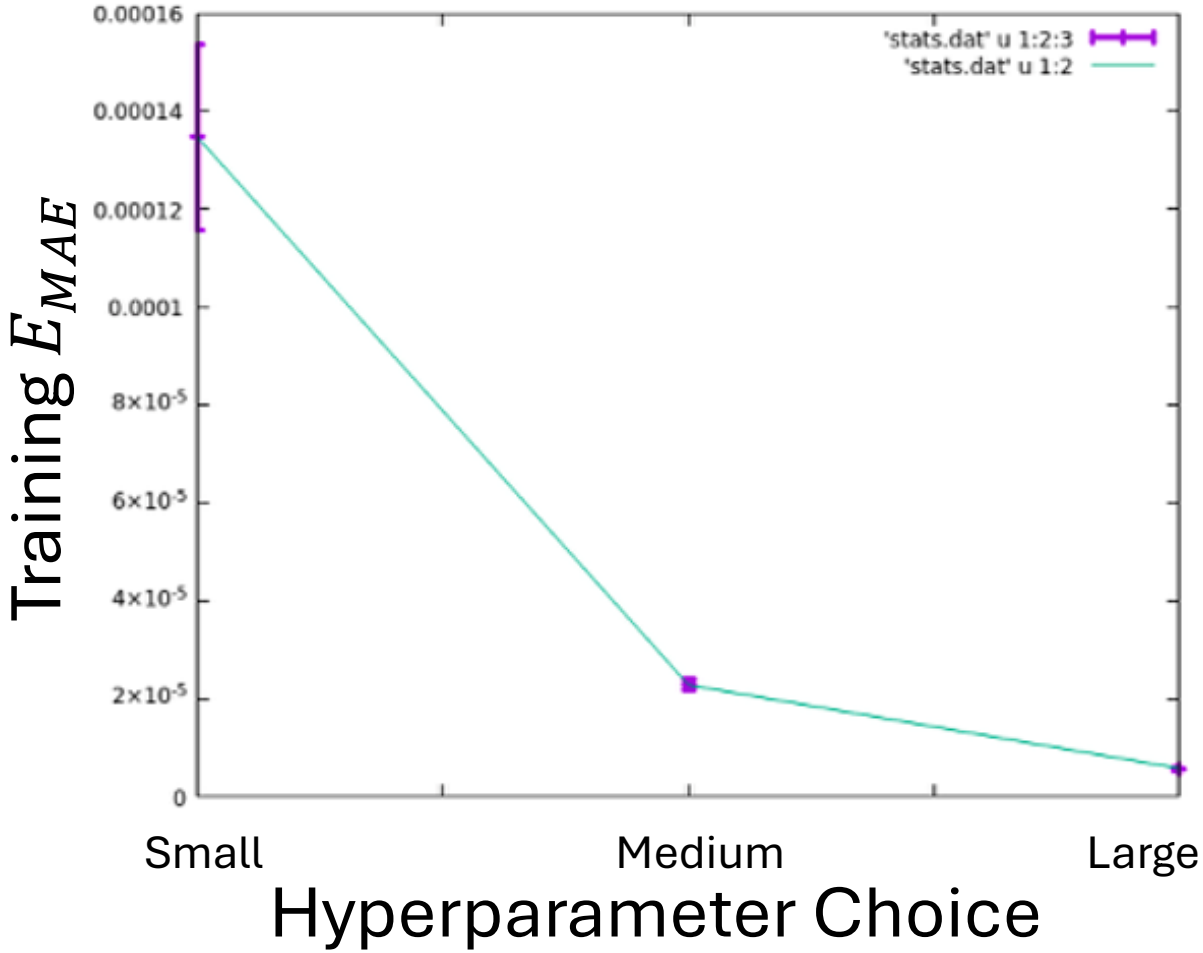

Project II Allegro Assessment: MD Stability

- In general, using Allegro model potentials for molecular dynamics simulations in LAMMPS is quite stable and fast
- We see within the NVE ensemble, energy and temperature are both well controlled over long simulation times of 2.8 ns
- Running on CPUs, these trajectories are reproducible
- Note the scale difference: temperature fluctuations are ~5x larger than energy fluctuations

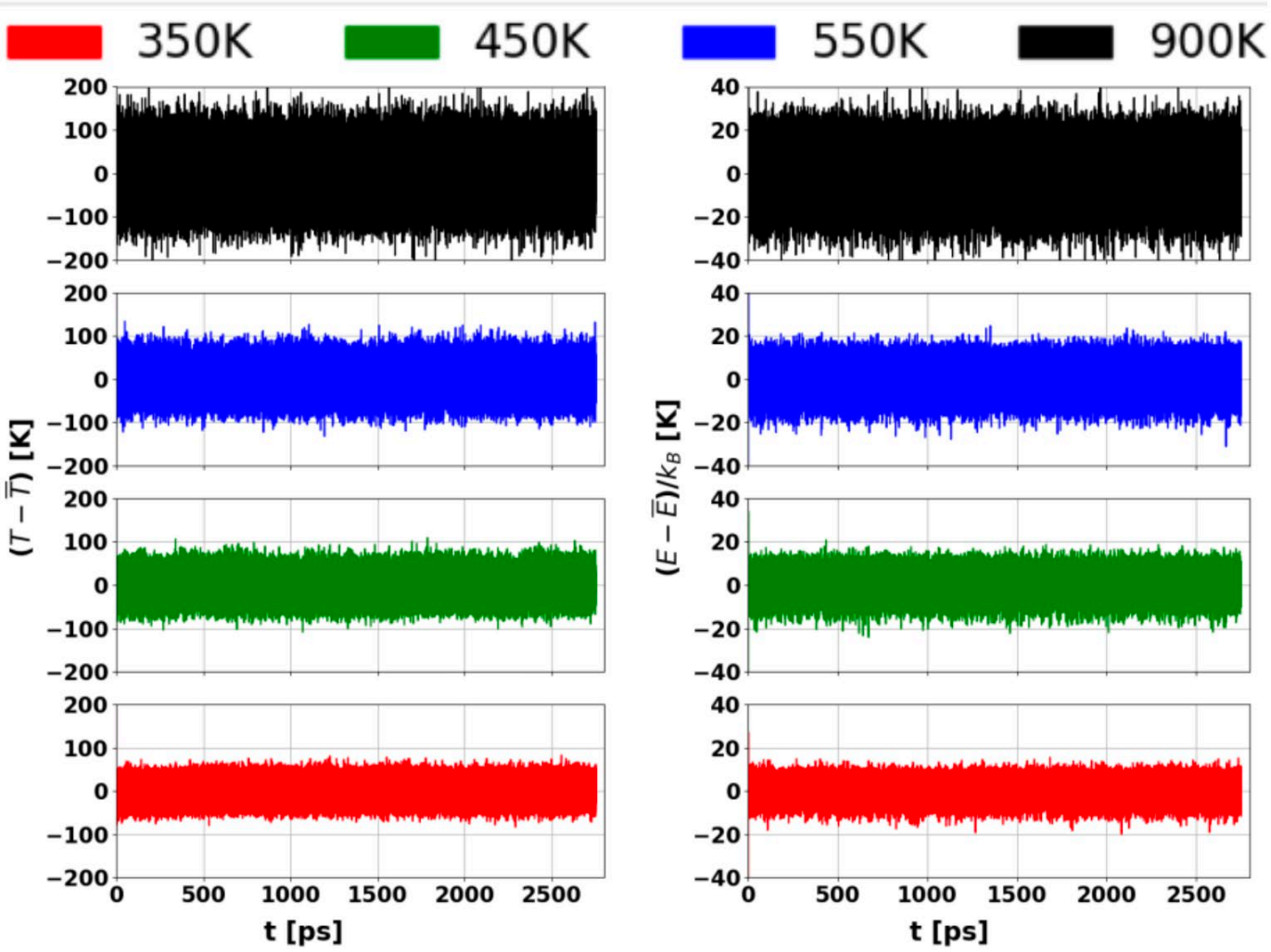

Project II Allegro Assessment: MD Instability

- Unfortunately, random infrequent stability issues may surface
- This seems to occur more readily at high temperatures
- We use a 900K screening test to filter out models which exhibit this issue
- Interestingly, “unstable” models otherwise seem to be well trained

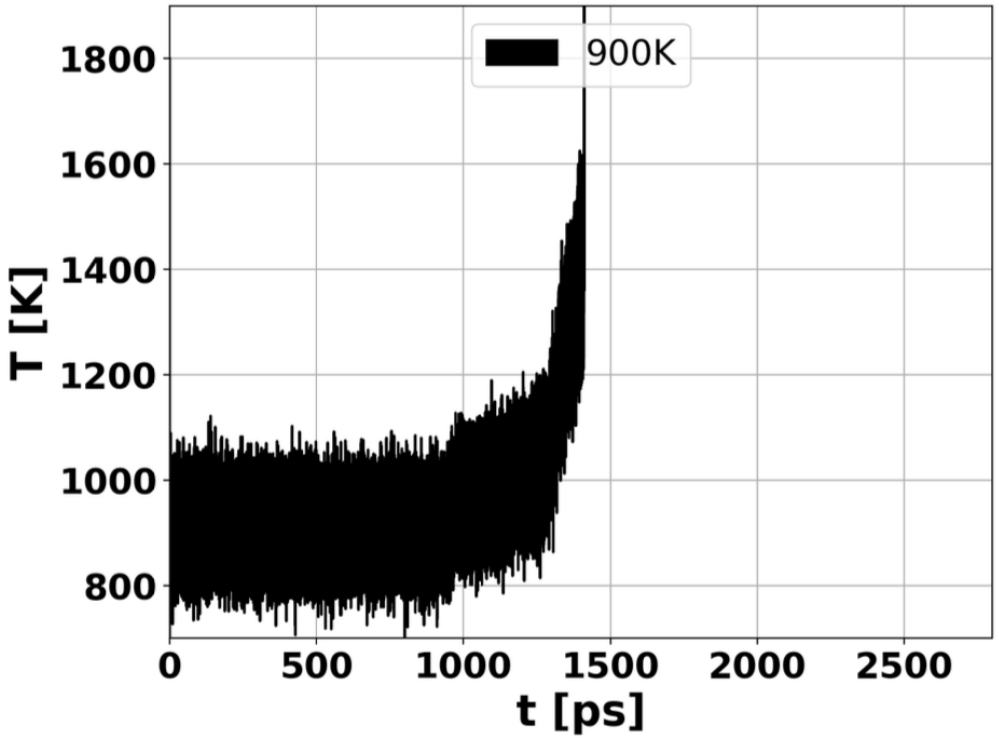

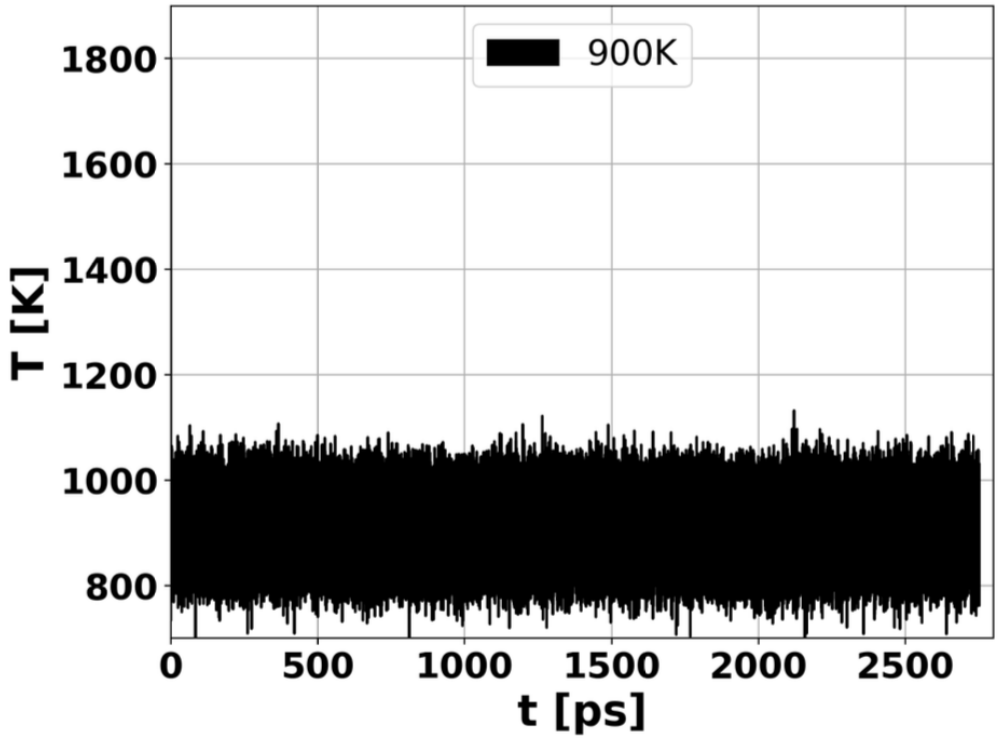

Project II Allegro Assessment: Close Pair Dataset

- The instability is not indicative of a poor model overall: it shows the limitations of the model's interpolative range
- This seems to be a result of atoms getting "too close", where the model fails to interpolate well to the close distance
- This interpolative failure results in catastrophic unphysical predictions of large forces/energies for the system
- Research is being done to mitigate this
- We have attempted to control this with qualitative success by constructing "close pair" configurations to add to the training and validation datasets

Assume framework is stationary, focus on Li atoms
For every Li - X and X - Li pair:
- move atom 1 towards atom 2 in discrete steps
- stop when atom1 & atom 2 PAW orbitals overlap
- exclude config if any other PAW orbitals overlap

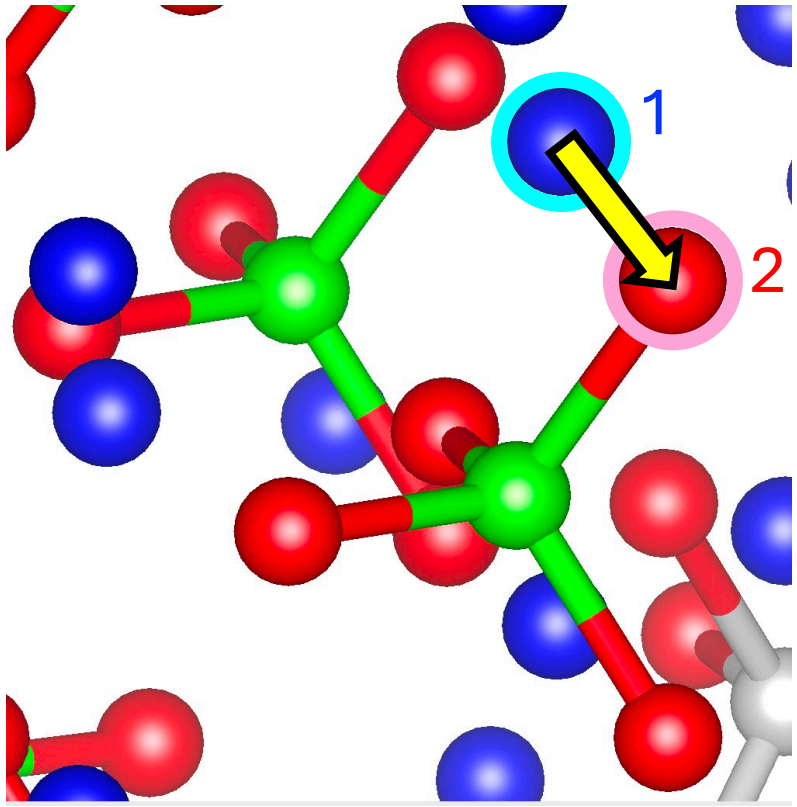

Project II Allegro Assessment: Model Training

- For our testing, we defined 10 models seen here
- Combined training on S1 and S2 increases dataset “diversity”
- Included 2 single structure training models for comparison
- Mostly focused on small models, included 2 medium models for comparison
- Models highlighted in red indicate 900K screening failures

Label	Model Size	Training Structure(s)	Best Epoch	Final Epoch	Stopping Type
CS1	Small	S1 + S2	160	660	plateau
CS2	Small	S1 + S2	11337	11401	timeout
CS3	Small	S1 + S2	8789	9123	timeout
CS4	Small	S1 + S2	798	1298	plateau
CS5	Small	S1 + S2	8220	8720	plateau
CS6	Small	S1 + S2	142	642	plateau
CM1	Medium	S1 + S2	10924	10934	timeout
CM2	Medium	S1 + S2	7967	8053	plateau
SS1	Small	S1	11955	12399	timeout
SS2	Small	S2	12426	12465	timeout

Project II Allegro Assessment: Model Metrics

- Training behavior and model size may have an impact on the error metrics
- No obvious link to 900K screening ”failures” and training results/errors
- Metrics overall are similar, have negligible impact

$$\mathrm{WS}^D = \frac{1}{3}\left(E^D_{\mathrm{MAE}} + F^D_{\mathrm{MAE}} + S^D_{\mathrm{MAE}}\right)$$

$$E^D_{\mathrm{MAE}} = \frac{1}{N_C}\sum_{\alpha=1}^{N_C}|\hat{E}_\alpha - E_\alpha| \quad F^D_{\mathrm{MAE}} = \frac{1}{3N_CN_A}\sum_{\alpha=1,\beta=1,\gamma=1}^{N_C,N_A,3}|\hat{F}_{\alpha,\beta,\gamma} - F_{\alpha,\beta,\gamma}| \quad S^D_{\mathrm{MAE}} = \frac{1}{9N_C}\sum_{\alpha=1,\gamma=1}^{N_C,9}|\hat{S}_{\alpha,\gamma} - S_{\alpha,\gamma}|$$

Model	WS^{train}	E^{train}_{MAE}	F^{train}_{MAE}	S^{train}_{MAE}
CS1	284.52	834.94	18.10	0.50
CS2	18.31	43.92	10.84	0.18
CS3	16.16	37.88	10.40	0.19
CS4	115.67	332.15	14.50	0.37
CS5	14.46	32.78	10.41	0.18
CS6	319.92	940.03	19.07	0.65
CM1	9.84	24.61	4.79	0.12
CM2	9.58	23.66	4.96	0.12
SS1	25.78	65.91	11.21	0.22
SS2	21.70	53.92	10.99	0.19

Model	WS^{val}	E^{val}_{MAE}	F^{val}_{MAE}	S^{val}_{MAE}
CS1	13.28	22.51	17.00	0.34
CS2	8.29	14.01	10.67	0.17
CS3	8.27	14.13	10.51	0.17
CS4	11.92	21.71	13.79	0.25
CS5	8.09	13.71	10.41	0.17
CS6	13.80	23.18	17.70	0.54
CM1	3.64	5.89	4.92	0.10
CM2	3.86	6.39	5.08	0.10
SS1	9.02	15.48	11.41	0.18
SS2	8.60	14.68	10.97	0.17

Project II Allegro Assessment: Minimize Results

- QE predicts lowest energy structure with structural relaxation calculation
- In LAMMPS, we can input this structure and perform a similar calculation
- This tests the Allegro model's ability to correctly find the same minimum energy structure as predicted by QE using DFT calculations
- Lower structural volume and energy change in LAMMPS indicate better agreement
- We see an observable trend between agreement with DFT and Allegro validation set error

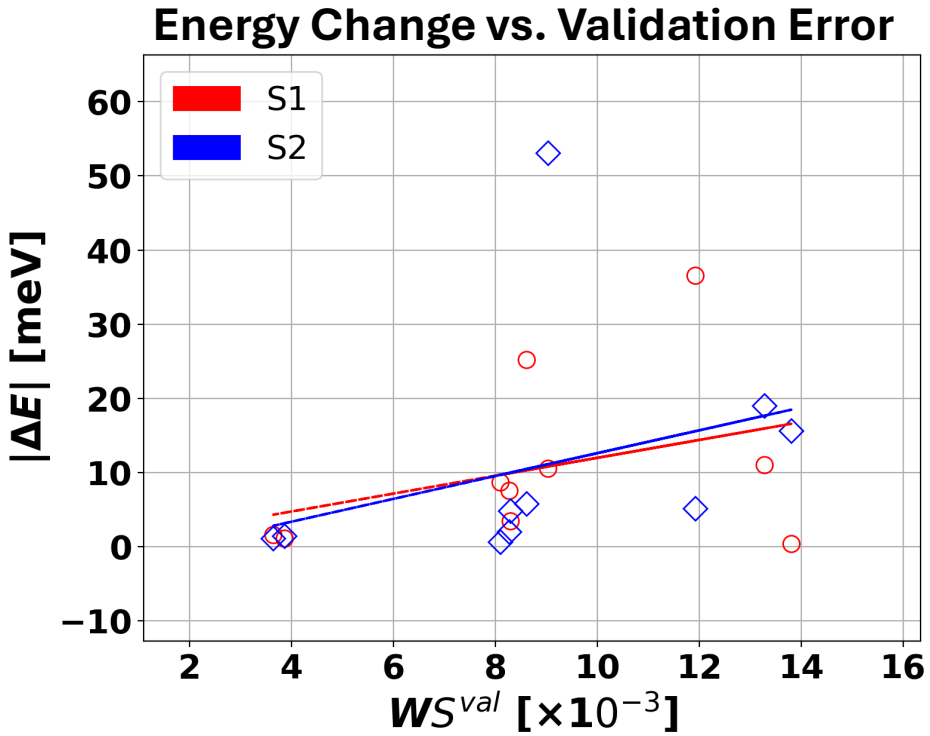

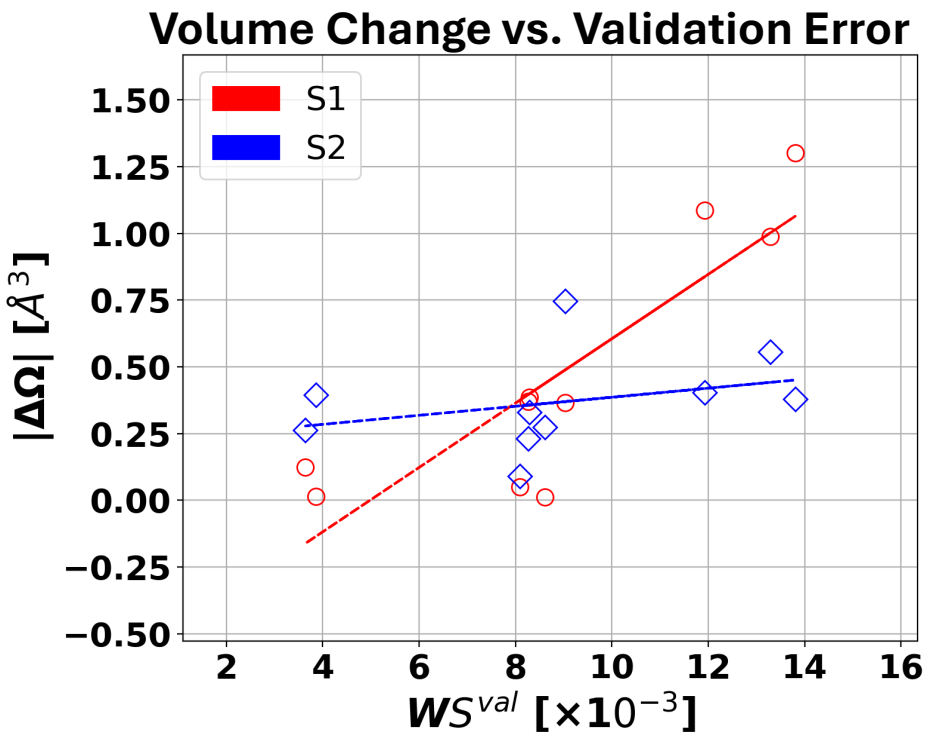

Project II Allegro Assessment: MD Simulations I

- ”Single averaging” – Block averaging of individual simulations
- CS2 model S1 results: 10 simulations with different initial atomic velocities
- 350K, 450K, and 550K with full (left) and tracer (right) interval functions
- We see 550K curves not well controlled, tracer is better controlled than full
- Errors of the individual interval functions are quite small (negligible)

$$\overline{\Lambda}^{\text{full}}_{\Phi,v}(\tau) = \frac{q_D^2}{6k_B\Omega}\frac{1}{\tau}\left\langle \left| \sum_{i\in D} \mathbf{r}_i(\tau) - \mathbf{r}_i(0) \right|^2 \right\rangle$$

$$\overline{\Lambda}^{\text{tr}}_{\Phi,v}(\tau) = \frac{q_D^2}{6k_B\Omega}\frac{1}{\tau}\left\langle \sum_{i\in D} \left| \mathbf{r}_i(\tau) - \mathbf{r}_i(0) \right|^2 \right\rangle$$

$$\overline{\sigma T}\rfloor^{\chi}_{\Phi,v} = \lim_{\tau\to\infty} \overline{\Lambda}^{\chi}_{\Phi,v}(\tau)$$

$\overline{\Lambda}^{\text{full}}_{\text{CS2,v}}(\tau)$ for Struct S1

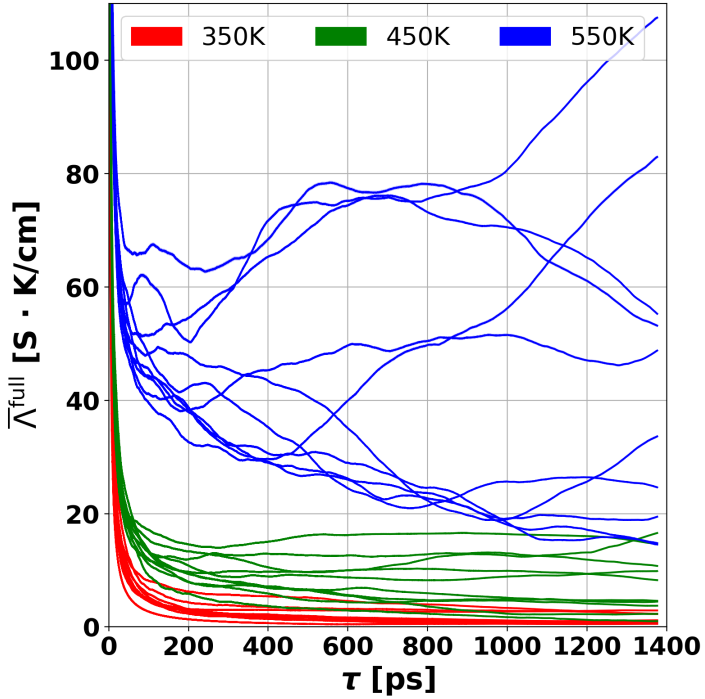

$\overline{\Lambda}^{\text{tr}}_{\text{CS2,v}}(\tau)$ for Struct S1

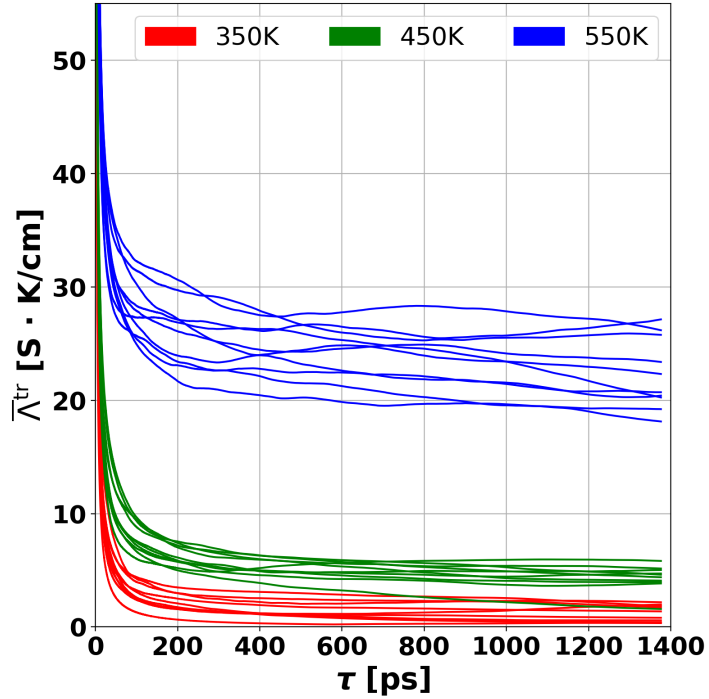

Project II Allegro Assessment: MD Simulations II

- "Double averaging" – additionally averaging over the 10 simulations
- Interval functions overall have better behavior at large τ limit (asymptotic)
- Errors are much more prominent as a result of the large spread seen earlier
- Again, 550K seems not well controlled, tracer is better controlled than full

$$\overline{\overline{\Lambda}}^{\text{full}}_{\Phi}(\tau) \equiv \frac{1}{v_T}\sum_{v=1}^{v_T}\overline{\Lambda}^{\text{full}}_{\Phi v}(\tau)$$

$$\overline{\overline{\Lambda}}^{\text{tr}}_{\Phi}(\tau) \equiv \frac{1}{v_T}\sum_{v=1}^{v_T}\overline{\Lambda}^{\text{tr}}_{\Phi v}(\tau)$$

$$\overline{\overline{\sigma T}}\rfloor^{\chi}_{\Phi} = \lim_{\tau\to\infty}\overline{\overline{\Lambda}}^{\chi}_{\Phi}(\tau)$$

$\overline{\overline{\Lambda}}^{\text{full}}_{\text{CS2}}(\tau)$ for Struct S1

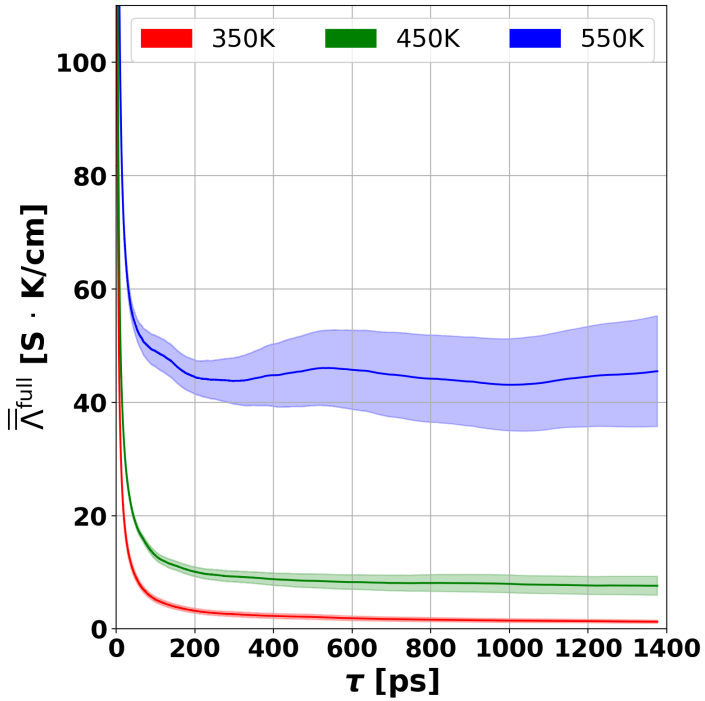

$\overline{\overline{\Lambda}}^{\text{tr}}_{\text{CS2}}(\tau)$ for Struct S1

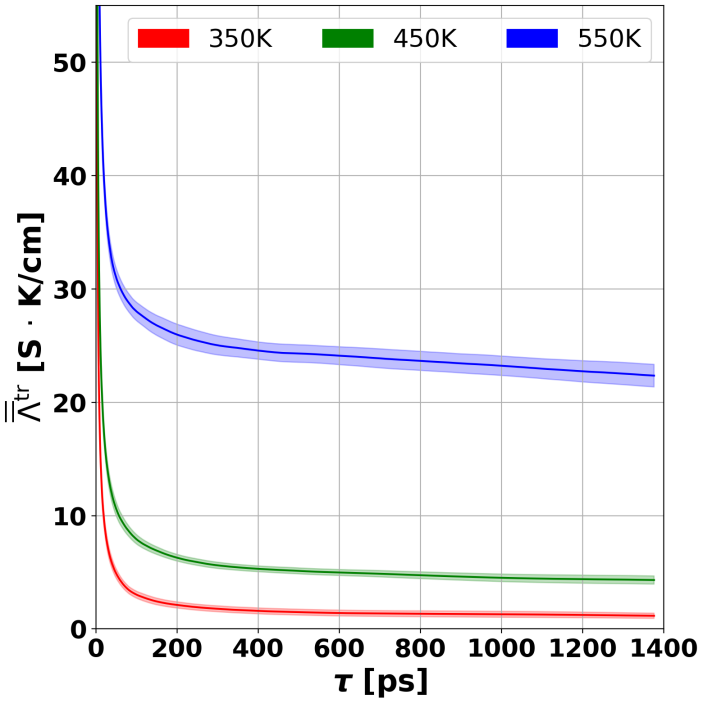

Project II Allegro Assessment: MD Simulations III

- We can now look at the double averaged interval functions for the 5 small combined training Allegro models
- We see that in general, the models are quite similar, except at 550K
- This showcases that high temperature is not well controlled
- Lower temperatures are better controlled, are realistic operational temps

$\overline{\overline{\Lambda}}^{\mathrm{full}}_{\Phi}(\tau)$ for Struct S1

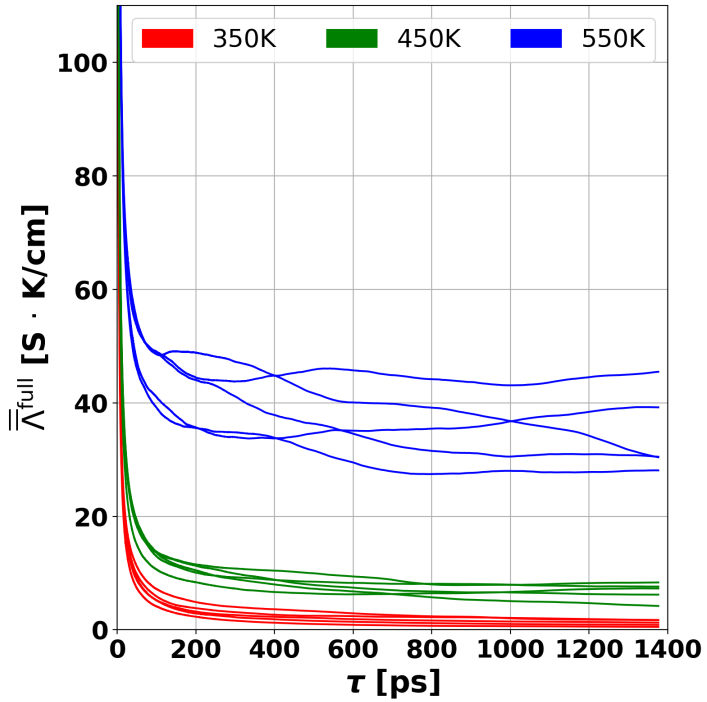

$\overline{\overline{\Lambda}}^{\mathrm{tr}}_{\Phi}(\tau)$ for Struct S1

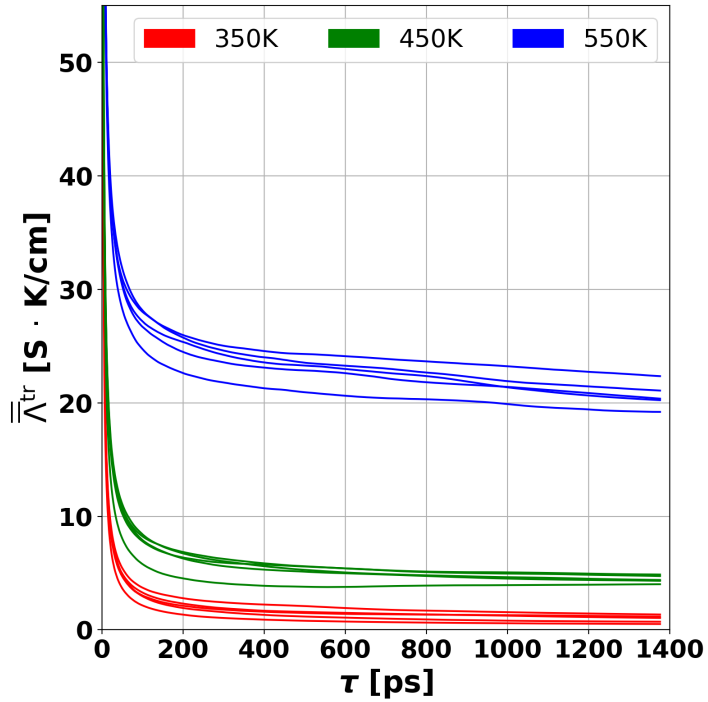

Project II Allegro Assessment: MD Simulations IV

- ”Triple averaging” – additionally average over the similar Allegro models
- Note that the large errors are again present at 550K
- Error magnitudes are similar to double averaged CS2 model
- Allegro model variability is much smaller than initial velocity variability

$$\overline{\overline{\Lambda}}^{\text{full}}(\tau) \equiv \frac{1}{N_\Phi} \sum_{\Phi=1}^{N_\Phi} \overline{\overline{\Lambda}}_\Phi^{\text{full}}(\tau)$$

$$\overline{\overline{\Lambda}}^{\text{tr}}(\tau) \equiv \frac{1}{N_\Phi} \sum_{\Phi=1}^{N_\Phi} \overline{\overline{\Lambda}}_\Phi^{\text{tr}}(\tau)$$

$$\overline{\overline{\overline{\sigma T}}}\rfloor^{\chi} = \lim_{\tau \to \infty} \overline{\overline{\Lambda}}^{\chi}(\tau)$$

$\overline{\overline{\Lambda}}^{\text{full}}(\tau)$ for Struct S1

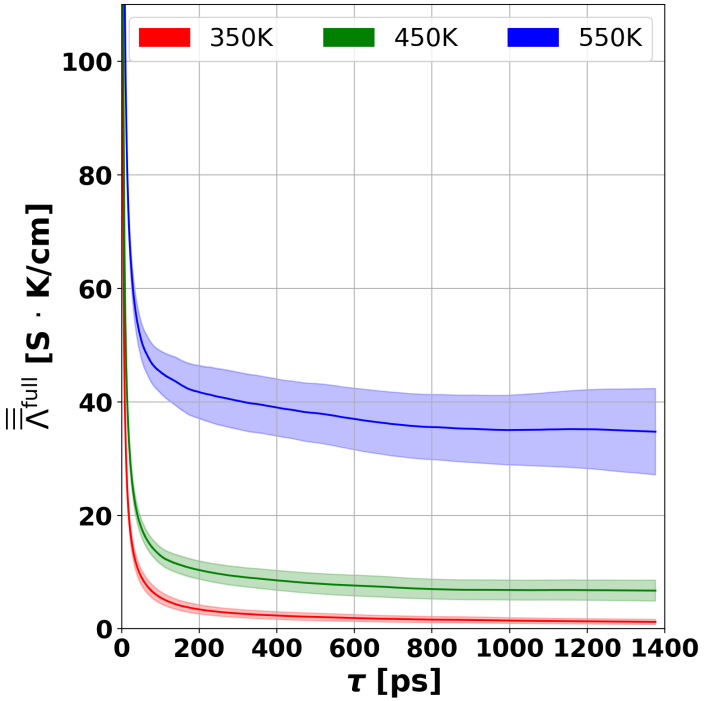

$\overline{\overline{\Lambda}}^{\text{tr}}(\tau)$ for Struct S1

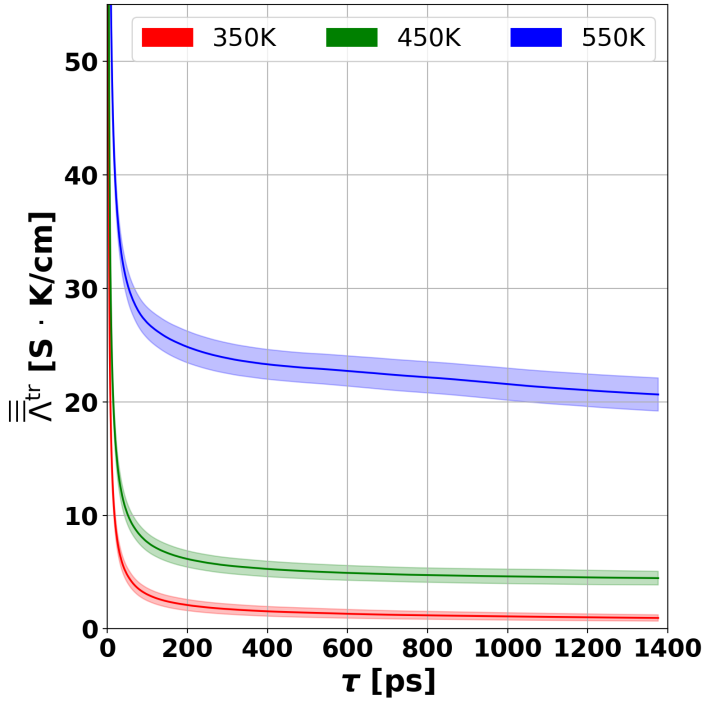

Project II Allegro Assessment: MD Simulations V

- Overall, the models have similar full interval function behavior
- SS1 and SS2 are similar

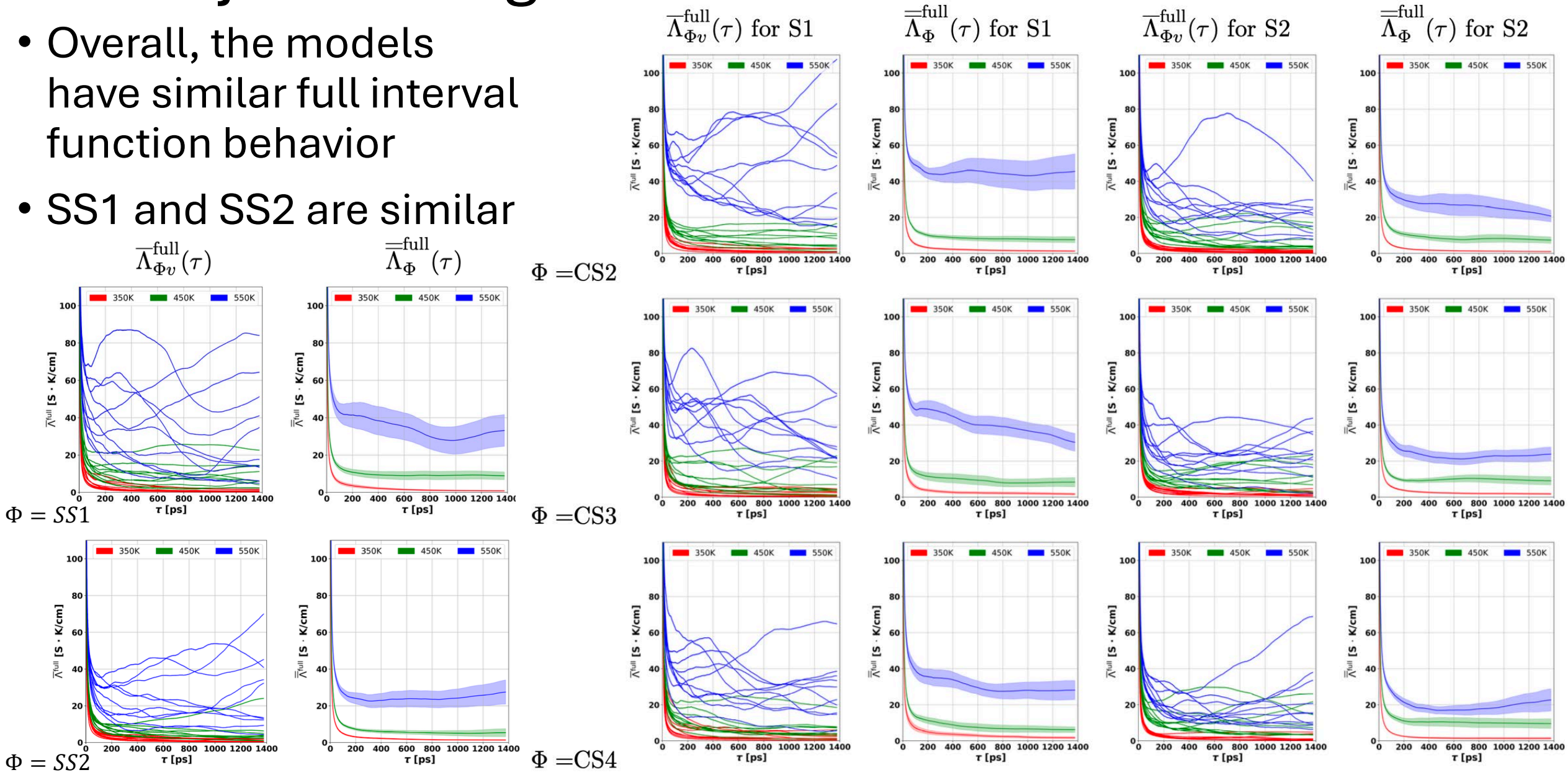

Project II Allegro Assessment: Conductivity I

- Conductivity is estimated by fitting interval functions to $f(\tau)$ and taking $\tau \to \infty$ limit
- Arrhenius plots of the 5 small combined (S1 + S2) models for structure S1
- Fits to the conductivity vs. temperature data vary widely across models
- This is due to small number of temperature data being fit (just 3 temperatures)
- This impacts the activation energy estimation, which is currently very rough

$$\overline{\overline{\sigma}}^{\chi}_{\Phi} \approx \lim_{\tau\to\infty} \frac{f^{\chi}(\tau)}{\overline{\overline{T}}_{\Phi}} \equiv \frac{f^{\chi}_{0}}{\overline{\overline{T}}_{\Phi}}$$

$$\overline{\overline{\sigma}}^{\chi} \approx \lim_{\tau\to\infty} \frac{f^{\chi}(\tau)}{\overline{\overline{T}}} \equiv \frac{f^{\chi}_{0}}{\overline{\overline{T}}}$$

$$\sigma T = C_0 \exp\left(-\frac{E_a}{k_B T}\right)$$

Full Conductivity (S1)

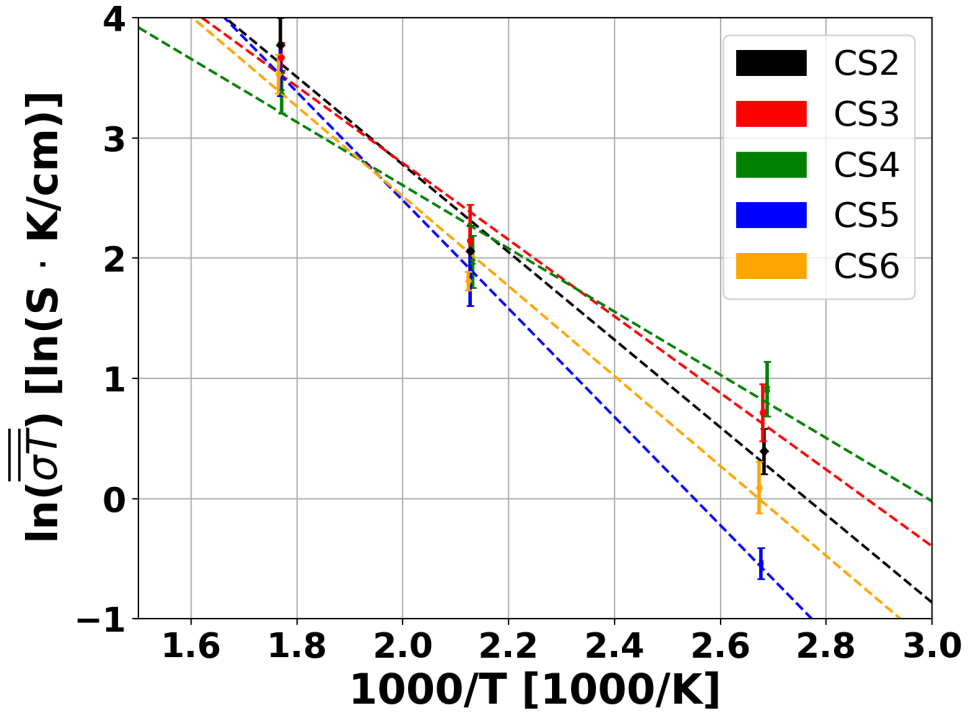

Tracer Conductivity (S1)

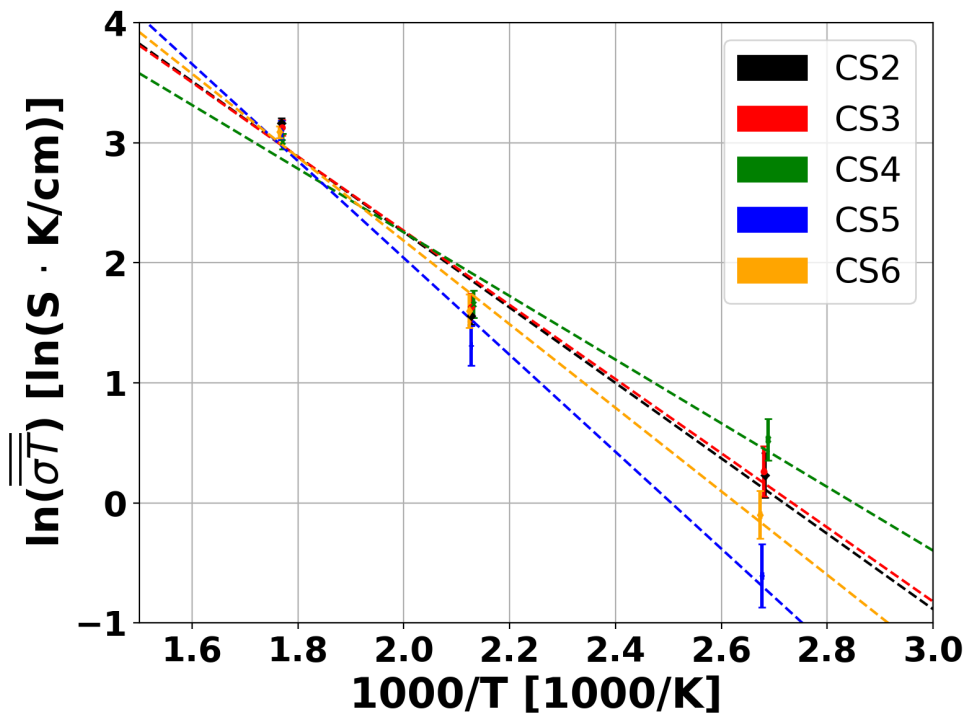

Project II Allegro Assessment: Conductivity II

- Can use Arrhenius plots to compare single models to combined model average
- Single models agree very well with the combined average, suggesting improving training “diversity” does not negatively impact single structure predictions
- We also see that overall, the full conductivity is higher than tracer, implying ionic correlations significantly contribute to the conductivity and cannot be ignored

Structure S1

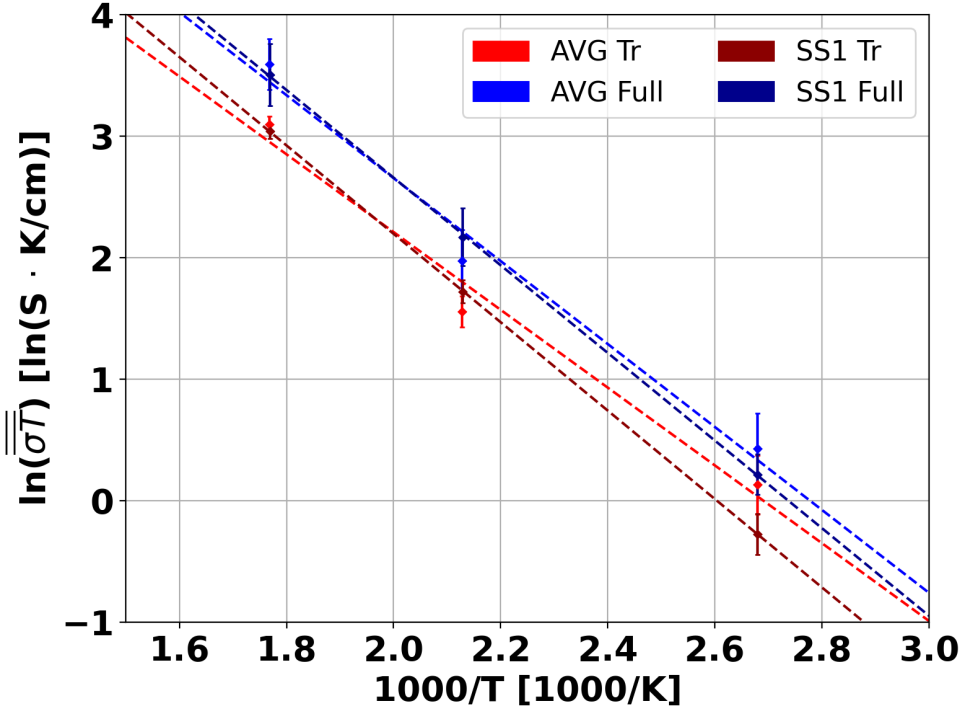

Structure S2

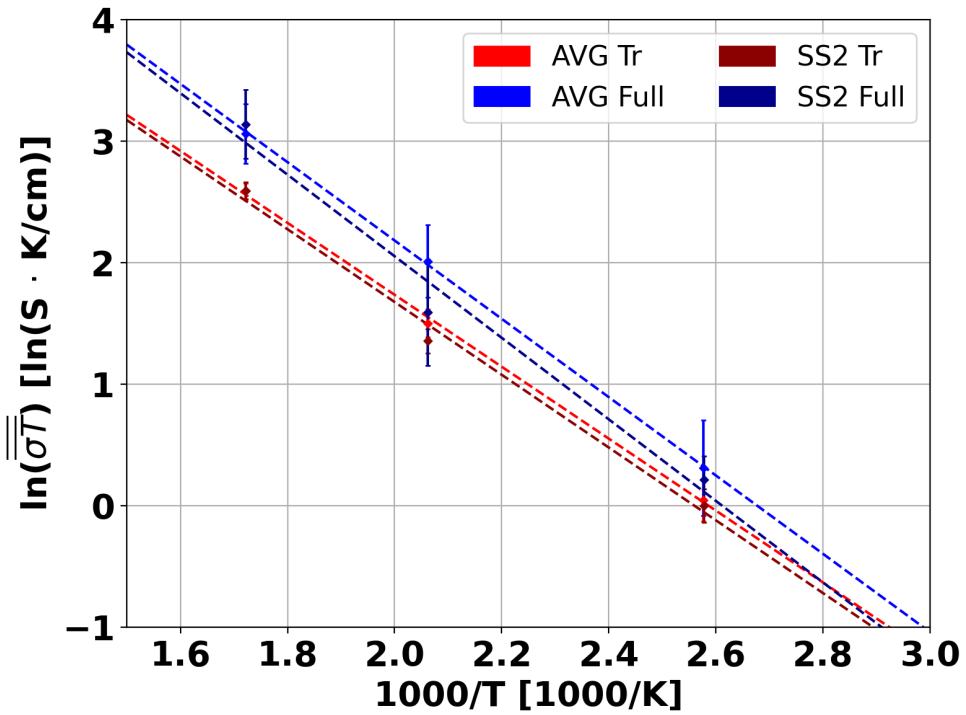

Project II Allegro Assessment: Summary

- Testing of Allegro architecture proved quite successful
- Low error metrics suggest good interpolation and agreement with DFT
- Can now run nanosecond MD simulations in just a few days!
- Longer simulations allow for excellent block averaging error
- High temperature interval functions still not well-behaved
- Low temperature interval functions well converged, can estimate σ_{GK}
- Significant variance/error with regards to velocity distributions
- Need to sample many more velocity distributions
- Can also imagine using larger unit cells with more atoms
- Small (but non-trivial) error associated with Allegro model initialization
- Good protocol to train a few Allegro models with different initializations
- Combined models agree with single models
- Combined training increases diversity, doesn’t affect single structure precision

Project III: Continued Study of (Thio) Boracites

- Successful Allegro assessment allows us to continue boracite study
- Can we train on individual materials and accurately calculate ionic conductivity in agreement with previous computation and experiment?
- Can we utilize these simulations to study ion migration mechanisms?
- Can we train with different stoichiometries/structural symmetries together?
- Can we confidently predict ionic conductivity for candidate materials?
- Can we assess the impact of larger numbers of initial velocity distributions?
- Can we assess the impact of larger simulation cell sizes?

Conclusions

- We were able to determine low energy structures for 8 known and predicted (thio)boracite materials, including new monoclinic Cc
- Determined all 8 materials are dynamically stable with phonon analysis
- Were able to show that Allegro can be used for low temperature estimates of the full ionic conductivity from long md simulations
- High temperatures not well controlled overall, but also not physical
- Initial velocity distributions contribute large error, but block averaging and Allegro model variance is well controlled
- Combined structure training improved diversity without negative impact on single structure predictions
- We are currently in early stages of applying what we learned from Allegro study to investigate the (thio)boracite ionic conductivities

Questions